2010

KLF2/KLF4 Double Knock-out Mouse Embryos Show Cranial Bleeding with Endothelial Disruption of the Primary Head Vein

Benjamin Curtis
Virginia Commonwealth University

KLF2/KLF4 Double Knock-out Mouse Embryos Show Cranial Bleeding with Endothelial Disruption of the Primary Head Vein

A thesis submitted in partial fulfillment of the requirements for the degree of Master of Science at Virginia Commonwealth University.

by

Benjamin Christopher Curtis
Bachelor of Arts, University of Virginia, 2008

Co-director: Jack L. Haar, PhD
Department of Anatomy and Neurobiology

Co-director: Joyce A. Lloyd, PhD
Department of Human and Molecular Genetics

Virginia Commonwealth University
Richmond, Virginia
August 6, 2010

Acknowledgments

Above all, I would like to extend my deepest gratitude to my two mentors, Dr. Jack Haar and Dr. Joyce Lloyd. Having the opportunity to be aided and guided by two very knowledgeable, thoughtful, and constructive people of very different scientific backgrounds has proved very rewarding. The two provided ongoing valuable advice, direction, and the timely offering of moral support throughout the course of my project, while injecting and re-injecting "undiminished enthusiasm." My understanding of scientific research and its clinical applications has been thoroughly strengthened and infused with a healthy dose of scientific skepticism. I thank Dr. Michael Fox for his role as an essential committee member and for his help with the in-situ hybridization protocol.

Second, I thank the well-learned team of graduate students and technicians, all of whom I consulted on a daily basis with questions and calls for assistance. Specifically, I thank Mohua Basu, who would jump over backwards to lend a daily helping hand. I thank Divya Vinjamur, with whom I would go to when troubleshooting technical problems. I thank Aditi Chiplunkarar, who took time to teach me new techniques. I thank Yousef Alhashem, who presented solid advice and gifted me with the hope that I can always better organize my surroundings. I thank Christopher Pang, the undergraduate student with wisdom and knowledge beyond his years, for providing insight and assistance with mice handling. I thank Anting Hsiung, who diligently helped me with the execution of the in-situ method. I also thank the numerous undergraduate students that aided in ways both big and small towards the completion of my project.

Third, I thank Sue Walker, Judy Williamson, and Dr. Jianmin Su of the Department of Anatomy and Neurobiology for their assistance with histological techniques and for the use of their reagents and supplies.

A special thanks is due to Aditi Chiplunkar, Gabriel Eades, Megan Smith, and Sean Fox for starting me off with a promising project. No doubt, after I have graduated, another long line of students will take up the KLF2/KLF4 torch.

Lastly, I thank my family and close friends for their moral support during my years of study, and for their understanding and flexibility when adapting their plans to accommodate the rather inconsiderate mating schedules of mice.

Table of Contents

List of Tables

Page

List of Figures

Page

List of Abbreviations

Adm……	adrenomedullin
Ang……	angiopoietin
BrA……	branchial arches
BMP……	bone morphogenic protein
bp……	basepair
cDNA……	complementary DNA
ChIP……	chromatin immunoprecipitation
chr……	chromosome
DEPC……	diethyl pyrocarbonate
DKO……	double knockout
DNA……	deoxyribonucleic acid
E8.5……	embryonic day 8.5
E9.5……	embryonic day 9.5
E10.5……	embryonic day 10.5
ECM……	extracellular matrix
Edn1……	endothelin 1
EfnB2……	ephrin-B2
End……	endothelial cell
eNOS…….	endothelial nitric oxide synthase
Ep……	epithelial cell
EpoR……	erythropoietin receptor
EphB4……	ephrin type-B receptor 4

ERG……	Ets related gene
Ery……	erythroid cell
GPA……	glycophorin A
GAG……	glycosaminoglycan
HUVEC……	human umbilical vein endothelial cell
H_2O……	water
Jag1 ……	jagged 1
kb……	kilobase pair
KLF……	Krüppel-like Factor
KLF2……	Krüppel-like Factor 2
KLF4……	Krüppel-like Factor 4
KO……	knockout
MCP-1……	monocyte chemotactic protein 1
MEF……	mouse embryonic fibroblast
$MgCl_2$……	magnesium chloride
mL……	milliliter
mM……	millimolar
MCP-1……	monocyte chemotactic protein 1
mRNA……	messenger RNA
Notch1……	notch homolog 1
Notch4……..	notch homolog 4
NRP1…….	neuropilin 1
NRP2…….	neuropilin 2

PBS…… phosphate buffered saline

PCR……. polymerase chain reaction

PDGFB…… platelet-derived growth factor beta

PDGFR…… PDGF receptor

PGK…… phosphoglycerate kinase

PI3K…… phosphatidylinositol 3-kinase

qRT-PCR…… quantitative reverse transcriptase polymerase chain reaction

RNA…… ribonucleic acid

rpm…… revolutions per minute

Scl…… Stem cell leukemia protein

TAE…… tris-acetate-EDTA

TGF…… transforming growth factor

TIE1…… tyrosine kinase with immunoglobulin-like and EGF-like domains 1

TIE2…… tyrosine kinase with immunoglobulin-like and EGF-like domains 2

TM…… thrombomodulin

U……. unit

µg…… microgram

µL…… microliter

VEGF…… vascular endothelial growth factor

VEGFR…… vascular endothelial growth factor receptor

VEGFR2…… vascular endothelial growth factor receptor 2

WT……. wild type

YS…… yolk sac

Abstract

Krüppel-like factors (KLFs) are a family of 3 Cys2/His2 zinc finger transcription factors with a diverse set of roles in cellular differentiation, cell cycle regulation, tumor suppression, erythropoiesis, angiogenesis, and other processes. During embryonic development, KLF2 has a role in vessel maturation. Adult conditional KLF4 knockout mouse embryos have thickened arterial intima follow vascular injury. Breeding KLF2+/- and KLF4+/- mice resulted in the generation of KLF2/KLF4 double knockout (DKO) embryos. KLF2/KLF4 DKO embryos died by E10.5 with cranial bleeding. Using immunohistochemistry, embryo whole-mounts were examined for differences in gross vascularization between wild-type (WT), KLF2-/- and KLF2/KLF4 (DKO embryonic day 9.5 (E9.5) embryos. No obvious gross capillary abnormalities were noted in E9.5 KLF2/KLF4 DKOs, although the posterior cardinal vein appeared to narrow rostral to caudal in KLF2-/- and KLF2/KLF4 DKO embryos. Light and electronic microscopy were employed to investigate potential structural and ultrastructural phenotypes in KLF2/KLF4 DKO embryos. Microscopy confirmed hemorrhaging near and endothelial breaks in the primary head vein (PHV) in E9.5 KLF2/KLF4 DKOs (n=8) and E10.5 KLF2-/-KLF4+/- embryos (n=1). Electron micrographs illustrated a disrupted endothelium in KLF2/KLF4 DKOs with endothelial cells having filopodia-like projections. Surprisingly, KLF2-/- embryos had the presence of wider medial PHV endothelial gaps compared to WT at the electron micrograph level. Density counts revealed a 15% reduction in midline cranial mesenchyme at the level of hemorrhaging in KLF2/KLF4 DKOs compared to KLF2-/- (n=3). An in-situ hybridization localized KLF2 RNA expression to the endothelium of the PHV. A quantitative reverse transcriptase polymerase chain reaction assay revealed that the eNOS expression is synergistically regulated by KLF2 and KLF4, as a shared downstream target. It is

proposed that KLF2 and KLF4 share in the regulation of multiple gene targets, leading to early death by E10.5.

Chapter 1: Introduction

This section aims to familiarize the reader with background information relevant to the study. First, a review of vascular development in the mouse embryo is made with emphasis on the impact of select vasculogenesis, angiogenesis, and vascular maintenance genes. Second, Krüppel-like factor genes are discussed both broadly and in their known roles as vascular regulators. Third, previous work on Krüppel-like factor models is noted, and lastly, the aims of the study are presented.

Development of the vascular system

Vertebrates rely on a closed vascular system for the transport of solutes, cells, hormones, nutrients, and gases to support daily living and maintain homeostasis. Of all organ systems, the cardiovascular system is the first to be established during embryogenesis. Vasculogenesis begins in mesoderm at embryonic day 8.5 (E8.5) in the mouse and terminates in the formation of the capillary plexus and dorsal aorta (Haar, 1970; Risau, 1997). Mesodermal cells, arising through the process of gastrulation, form lateral mesoderm, intermediate mesoderm, paraxial mesoderm (somites) and axial mesoderm (notocord) (Murray, 1932). The first endothelial cells are formed in lateral and posterior mesoderm. This lateral and posterior mesoderm also migrates toward the yolk sac, a developing sheath attached to the embryo proper, and differentiates into endothelial and hematopoietic cells forming blood islands (Reviewed by Eichmann, 2005). A precursor cell, the hemangioblast, is able to differentiate into both endothelial and hematopoetic cells, as well as other lineages (Choi, 1998; Nishikawa, 1998). After the formation of blood islands, local endothelial cells anastomose, forming a primitive capillary network that functions as the first extraembryonic vascular system prior to the pumping of blood. At the same time, the dorsal

aorta and many capillaries have formed in the embryo proper through aggregation of endothelial cells, this time without the generation of hematopoietic counterparts. When the heart starts beating (around day 8.5 post-coitus in mice) a circulatory loop between yolk sac and embryo has formed, followed soon by remodeling of the yolk sac capillary plexus into arteries and veins (Reviewed by Eichmann, 2005). Blood that leaves the heart is pumped through the dorsal aorta, entering the yolk sac via the vitelline artery and its branches. To return to the heart, blood flows through the peripheral sinus vein and into the anterior venous plexus. Yolk sac hematopoietic cells differentiate into primitive erythrocytes through primitive erythropoiesis, followed days later by definitive erythropoiesis that starts in the yolk sac and continues in the fetal liver (Cumano, 2001).

To form a network of vessels that successfully perfuse the embryo, it is necessary for arterial-venous differentiation and a remodeling of vessels to meet changing nutrient requirements; that is, the embryo must undergo a process of angiogenesis, beginning around E8.5 – E9.0 (Reviewed by Carmeliet, 2000). During this process, vessels branch into avascular regions through the release of proteases that degrade the basement membranes of the parent vessels. Pericytes and smooth muscle cell progenitors surround the forming vessels, providing support **(**Reviewed by Carmeliet, 2000**)**. Capillaries connect and disconnect to support local requirements. If these capillaries fail to disconnect, the shunts formed lead to inadequate perfusion of peripheral tissue, such as yolk sac, followed by anemia and death (Reviewed by Eichmann, 2005).

The embryonic heart that circulates the vascular supply is formed beginning in early gastrulation around E7.25 when mesoderm of the anterior third of the primitive streak forms an early tubular heart (Sissman, 1970). As it develops, the heart pumps blood to support tissue

needs while gradually remodeling into four fully-formed chambers (Brand, 2003). At E9.5, the primary head vein (PHV) is visible in the primitive mouse head. The PHV drains three plexuses early in development: anterior plexus, middle plexus, and posterior plexus. Later, the anterior and middle plexuses anastomose (Cunningham, 1902). The anterior portion of the PHV transforms into the cavernous sinus, while the posterior portion disappears altogether, except for where it joins caudally with the anterior cardinal vein. These two vessel segments together form the internal jugular vein (Gray, 1923), which drains blood from the adult head.

Blood vessel composition

Endothelium is composed of simple squamous epithelium that lines the interior of the developing blood vessels. Endothelial cells have a unique set of functions, including documented roles in vasodilation, vasoconstriction, blood coagulation, leukocyte transmigration, inflammation, wound healing, atherogenesis, antigen presentation, leukocyte anchoring and lipoprotein metabolism (Gerritsen, 1987). Tissue-specific endothelial cells have additional functions. For instance, the blood-brain barrier is established through polarized endocytosis and transcytosis between endothelium and astrocyte endfeet (Abbott, 2002). Liver endothelial cells form fenestrated and discontinuous vessels, mediating the exchange of portal blood, toxins, and metabolites between Kuppfer cells and hepatocytes (Kmiec, 2001). While vessel fenestration in the developing mouse has not been well characterized, studies have reported that vessel fenestration may be induced through application of vascular endothelial growth factor (VEGF) in adult male rats (Roberts, 1995). The question has been asked: “Do microenvironments dictate the fate of endothelial cells?” For example, brain vasculature grafts, directed into peripheral tissue have a reduced number of tight junctions, typical of peripheral tissue; whereas, the number

rebounds when the vessels penetrate back through into native brain tissue (Stewart, 1981). Alternatively, heart tissue placed in the inner ear followed by observed vessel growth demonstrated the expression of Willebrand factor, typically only expressed in heart vasculature (Aird, 1997). Taken together, these experiments show that the roles and fates of endothelial cells are at least partially, but not completely, determined by their microenvironments, and that endothelial cells maintain some level of cell fate plasticity (Cleaver, 2003). Preliminary data displayed in the subsequent sections show vessel-specific endothelial disruption due to the ablation of two Krüppel-Like Factor genes.

Roles of crucial vascular development genes

In the development and maintenance of the vascular system, researchers have asked how the level of "cross-talk" between endothelial cells and surrounding tissue may dictate cellular functions. This "cross-talk" is possible through the expression and interaction of a variety of crucial vascular development genes. Figure 1 depicts a partial list of these genes and the stages at which they act. For instance, vascular endothelial growth factor (VEGF) of the VEGF family orchestrates the development of various vascular programs. Peripheral sensory nerves expressing VEGF provide a template for arteriogenesis and branching in mouse skin (Mukouyama, 2002); alveoli expressing VEGF pattern pulmonary vasculature formation (Ng, 2001); and VEGF-positive astrocytes guide vascularization of the retina in response to hypoxia (Stone, 1995). One of its receptors, VEGF receptor (VEGFR or Flt-1) is important in the assembly of vascular channels, with knockout models dying *in utero* at approximately E8.5. VEGFR mediates endothelial-to-endothelial cell interactions and matrix-to-endothelial cell interactions (Fong, 1995). VEGF Receptor 2 (VEGFR2 or Flk-1) knockout mice die 8.5 – 9.5

days post-coitus, failing to form yolk sac blood islands or to organize blood vessels in the embryo proper (Shalaby, 1995).

Another "cross-talking" ligand-receptor pair is platelet-derived growth factor (PDGF) and platelet-derived growth factor receptor (PDGFR). Endothelium secretes PDGF, (Zerwes, 1987), while mesenchyme, a smooth muscle progenitor, expresses PDGFR (Shinbrot, 1994). Mesodermal cells were shown to migrate towards endothelial cells *in vitro* when mediated by PDGF-B (Hirschi, 1998), while ablation of the PDGF-B gene in mice results in hemorrhaging, likely due to the reduced coverage of supporting pericytes (Leveen, 1994; Lindahl, 1997). In reverse fashion to PDGF-PDGFR binding the pairing can be switched, where the ligand is expressed by the mesenchyme and receptor by the endothelium.

Such is the case with angiopoietin-1 (Ang-1) and its receptor, endothelial receptor tyrosine kinase (Tie-2). Here, mesenchyme surrounding Tie-2 expressing endothelium secretes Ang-1, which stimulates Tie-2 on endothelial cells (Davis, 1996). The interaction leads to pericyte and smooth muscle recruitment, evidenced by vascular defects observed in the Ang-1-/- knockout model (Suri, 1996). Transgenic overexpression of angiopoietin-2 (Ang-2), a natural Ang-1 antagonist, disrupts blood vessel formation in the mouse embryo. Ang-2 is normally only expressed in areas of vessel remodeling (Maisonpierre, 1997). Tie-1-/- embryos lack endothelium structural integrity, resulting in edema and localized hemorrhaging (Sato, 1995).

In forming the vascular system, the developing embryo sends out signals that differentiate arterial and venous blood vessels. Transcription of Ephrin-B2, an eph family transmembrane ligand, has been localized to arteries alone, while its binding partner, Eph-B4, is a receptor tyrosine kinase found only in veins. Together, the two coordinate the molecular mechanism of arterial-venous differentiation (Wang, 1998).

Lastly, Transforming Growth Factor Beta (TGFβ) and its receptors likely play a role in angiogenesis. Targeted disruption of the TGFβ gene results in either early embryonic death around E10.5 due to vessel rupturing in the yolk sac or death 3 weeks after birth due to pulmonary edema (Dickson, 1996). Extensive research on TGFβ receptors reveals their importance in establishing and maintaining embryonic vasculature (Reviewed by Pepper, 1997). Unsurprisingly, both TGFβ and TGFβ receptors are found unregulated in cancer.

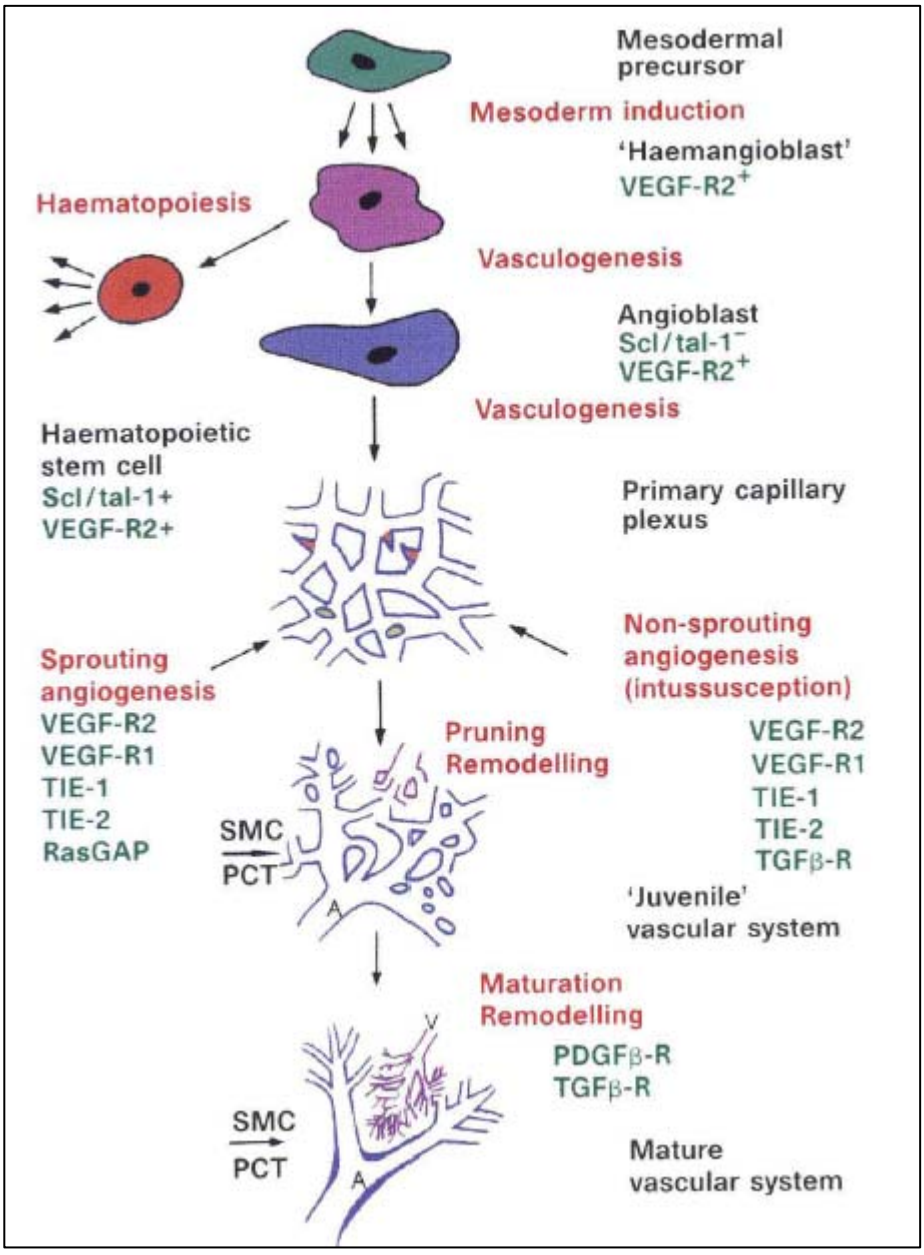

Figure 1: Process of vasculogenesis and angiogenesis. Red tips represent sprouts, yellow circles represent splitting pillars. A, arteriole; V, venule; SMC, smooth muscle cells; PCT, pericytes (Risau, 1997).

Krüppel-Like Factors

Krüppel-Like Factors (KLFs) are a family of 17 known DNA-binding proteins (KLF1-17) with sequence homology to the well-characterized *Drosophila* Gap gene, *Krüppel* . KLFs share three conserved C2/H2 zinc finger domains, together totaling 81 amino acid in length (Suske, 2005). Zinc finger motifs, first discovered in the *Xenopus* transcription factor TFIIIA, are formed through the coordination of histidine and/or cysteine to a central zinc cation (Brown, 1985, Miller, 1985). The cation bends the amino acid sequence back onto itself, forming the characteristic "finger" structure, which inserts itself into the DNA major groove (Pabo, 2001). KLFs have a conserved TGEKP(Y/F)X amino acid sequence, between each zinc finger (Dang, 2000). It has been proposed that during DNA-binding, KH(A/S) within the first finger, RER within the second, and RH(K/L) within the third zinc finger make the actual contacts to the DNA, binding to GC boxes and GT/CACCCC DNA binding motifs (Crossley, 1996; Matsumoto, 1998; Chen, 2009).

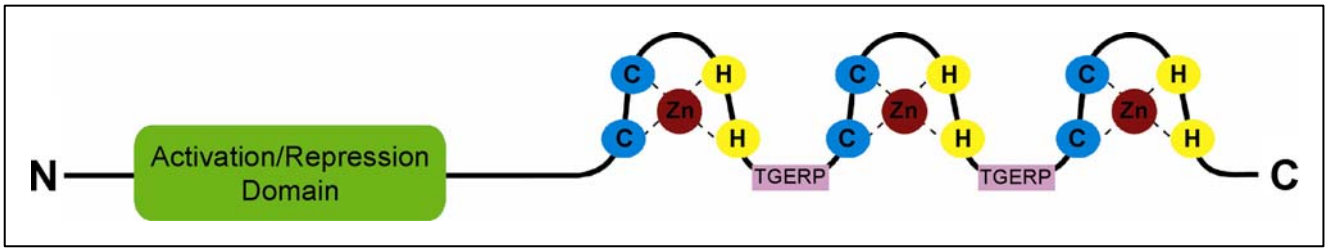

Figure 2: KLF C2/H2 zinc finger model. KLF Zinc fingers conform to the $CX_{2-4}CX_{12}HX_{2-6}H$ pattern above with critical cysteine and histidine amino acids coordinating to a central zinc cation. (Pearson, 2007)

KLFs can function as activators and repressors through separate trans-activating and trans-repressing protein domains located at the N-terminus of the molecule (Conkright, 2001). Erythroid Krüppel-Like Factor (EKLF or KLF1) was the first KLF to be identified, followed by Lung Krüppel-Like Factor (LKLF or KLF2) using a hybridization probe thought to be unique to the EKLF conserved zinc finger region, suggesting the existence of a larger, multigene family

(Anderson, 1995). Phylogenetic analysis has demonstrated that EKLF, KLF2, and Gut Krüppel-Like Factor (GKLF or KLF4) are about 90% similar in the zinc finger domain (reviewed by Philipsen, 1999, Bieker, 2001). These KLFs share a common 5 bp binding site, CACCC, and the expression level of target genes is impacted by the amount and orientation of these KLF-specific binding sites at the β-globin locus (Bieker, 1995; Chen, 2009). Due to high amino acid similarity in the DNA binding region, it was proposed that EKLF and KLF2 may regulate some shared gene targets *in vivo*. EKLF/KLF2 double knockout (DKO) mice were used to show that EKLF and KLF2 both positively regulate embryonic β-globin gene expression and are necessary for primitive erythropoiesis (Basu, 2007). Even more convincing, the DKO mice appear anemic at E10.5 and die by E11.5, earlier than KLF2-/- or EKLF-/- embryos. It was proposed that similar gene co-regulation might exist between the highly similar KLF2 and KLF4, and that generation of KLF2/KLF4 DKO embryos would have additional morphological defects in than either single knockout model.

Krüppel-Like Factor 2

Expression and Function of KLF2

KLF2 is located on mouse chromosome 8. KLF2 transcripts are highly expressed in the lungs and spleen of the adult mouse by Northern blot (Anderson, 1995) and can also be found in endothelial cells of the developing vasculature in mouse embryos at E9.5 by in-situ hybridization (Kuo, 1997). Analysis by quantitative reverse transcriptase polymerase chain reaction (qRT-PCR) revealed that KLF2 is expressed in both primitive and definite erythroid cells (Basu, 2004; Zhang, 2005). The KLF binding motif at the Nanog enhancer was examined by transfecting a construct containing a point mutation into embryonic stem (ES) cells. The ES cell tissue was

probed in an electrophoretic mobility shift assay (EMSA), the DNA-protein interaction suggesting that KLF2 and KLF4 may share the more stringent binding site sequence: CCRCCC (Jiang, 2008).

KLF2 is required for blood vessel stabilization, evidenced by knockout models discussed later. In the presence of PDGFβ, KLF2+/+ and KLF2+/- mouse embryonic fibroblasts (MEFs), a model for vascular smooth muscle cell (VSMC) migration, had increased migration in RPMI media compared to KLF2-/- MEFs, suggesting that KLF2 is necessary for smooth muscle cell migration (Wu, 2008). However, a recent study suggests that KLF2 may play a more complicated role during development. In this study, human umbilical vein endothelial cells (HUVECs) were infected with KLF2-GFP adenovirus to overexpress KLF2 and co-cultured with VSMCs. The KLF2-GFP co-culture had reduced VSMC migration in hydrogel scaffold compared to the HUVEC co-culture infected with control GFP adenovirus (Mack, 2009). As such, while KLF2 may have an important role in VSMC migration, its function as either a positive or negative regulator may be dependent on variables which are unknown at this time.

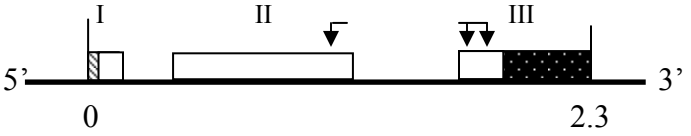

Figure 3: Structure of KLF2 gene on mouse chromosome 8. The boxes indicate exons, numbered with roman numerals, clear boxes indicate translated codons, the dashed boxes indicates the 5'UTR, the spotted box indicates the 3'UTR. The arrows indicate the three C2/H2 zinc fingers. Scale is given in kilobase pairs.

Knockout Models

KLF2 KO mice were produced using mouse embryonic stem (ES) cells, a targeting vector containing regions of the KLF2 gene, and an expression cassette of phosphoglycerate kinase (PGK) promoter-driven hypoxanthine phosphoribosyltransferase (HPRT) minigene. Through homologous recombination with the endogenous KLF2 gene, the vector deleted 2.2 kb, including

the KLF2 promoter region, the transcription activation domain, and a portion of the DNA binding domain, completely eliminating expression of KLF2 in mice homozygous for the deletion (Wani, 1998).

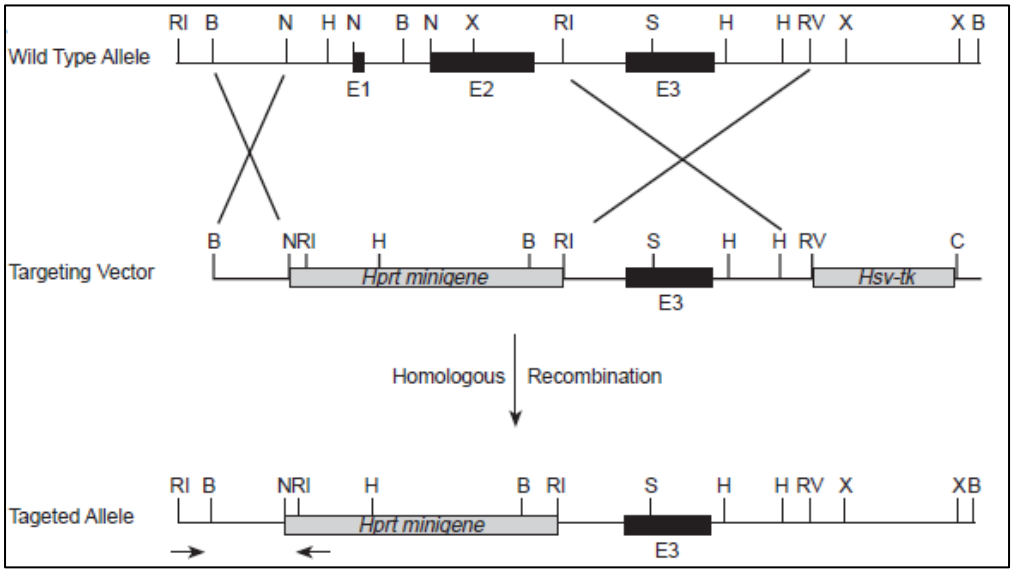

Figure 4: Disruption of KLF2 gene. KLF2 wild-type gene is recombined with Hprt minigene using a targeting vector, generating the KLF2 KO allele. Single letter abbreviations represent restriction enzyme cut sites (Wani, 1998).

The stem cells in which homologous recombination had taken place were then harvested, screened for the KLF2 gene deletion, and injected into blastocysts, and implanted in pseudopregnant mice. Mating the resulting heterozygotes generated the knockout mouse. It was observed that KLF2 KO mice died during gestation, demonstrating the essential role of KLF2 during development. At E12.5 KLF2 KO mice exhibited severe anemia, retarded growth, abdominal bleeding, and a poorly formed jaw. None survived beyond E13.5 (Wani, 1998). This KLF2 KO model was used in the experiments presented in this thesis.

Additional KLF2 KO mice were independently generated by another group at the University of Chicago. These researchers ablated KLF2 expression through insertion of a PGK-

driven *neomycin* cassette. Here, the entire KLF2 gene was replaced with the targeting construct (Kuo, 1997). These KLF2 KO embryos died between E12.5 – E14.5 due to severe intra-embryonic and intra-amniotic hemorrhaging. The umbilical veins and arteries of E12.5 KLF2 KO mice displayed reduced thickness of the tunica media, reduced extracellular matrix (ECM), fewer mural cells, accompanied by aneurysm and hemorrhage. The vessels contained both CD34-positive endothelial cells and αSMA-positive mural cells, indicating that KLF2 does not impact differentiation of these two cell lineages (Kuo, 1997).

In Tie2-Cre conditional KLF2 KOs, where KLF2 is selectively ablated in endothelial cells, embryos exhibited heart failure and died by E14.5 without any signs of hemorrhaging (Lee, 2006). At E11.5 these Tie2-Cre conditional KLF2 KO embryos had no significant difference in gene expression in tested common regulators of vasculogenesis, including endothelial nitric oxide synthase (eNOS), PDGFβ, PDGFR, tyrosine kinase with immunoglobulin-like and EGF-like domains 1 (Tie1), notch homolog 1 (Notch1), notch homolog 4 (Notch4), jagged1 (Jag1), ephrin-B2 (EfnB2), ephrin type-B receptor 4 (EphB4), adrenomedullin (Adm), endothelin 1 (Edn1), and erythropoietin receptor (EpoR). In another study, HUVEC cultures in which KLF2 is knocked down with siRNA showed decreased expression of eNOS compared to control and decreased repression of Edn1 and Adm compared to control (Dekker, 2005). The decrease in eNOS expression in KLF2 siRNA HUVEC culture not seen in KLF2 Tie-2 KOs may be due to the altered gene expression of an established cell culture compared to a functional animal model. Alternatively, it could illustrate how communication from other cell types and/or other factors effectively rescues expression of KLF2 target genes *in vivo*.

Regulation of KLF2

Shear stress in vasculature due to blood flow has been shown to upregulate both KLF2 and its downstream anti-inflammatory effectors (Dekker, 2002; Huddleson, 2004; van Thienen, 2006). Shear stress is typically low in atherosclerosis-vulnerable vasculature, and KLF2 upregulation in response to shear stress, occurs via the MEK5/ERK5/MEF2 signaling pathway (Parmar, 2005). Additionally, expression of phosphatidylinositol 3-kinase (PI3K) was shown to acetylate histones H3 and H4 in the KLF2 promoter via shear stress, using chromatin immunoprecipitation (ChIP) analysis and PI3K inhibitor, LY294002 (Huddleson, 2005). In addition, the same study used a luciferase reporter assay to demonstrate how a KLF2 gene tripartite palindrome motif drives the shear stress response.

KLF2 Downstream Effectors

KLF2 was shown to bind cooperatively with ERG (Ets related gene) protein to activate vascular endothelial growth factor receptor 2 (VEGFR2). An HA-tagged KLF2 and ERG co-immunoprecipitation assay were used to show interactions between the two proteins, while qRT-PCR analysis with simultaneous injection with ERG and KLF2 mRNA were used to show synergistic upregulation of VEGF2 in zebrafish embryos (Meadows, 2009). An earlier study suggested that KLF2 binds to the VEGFR2 promoter and inhibits its expression, resulting in a downregulation of VEGF-A mediated angiogenesis (Bhattacharya, 2005).

KLF2 has been implicated in a host of anti-inflammatory processes whose mechanistic characterization may ultimately hold therapeutic value. For example, KLF2 may play a role in statin-treatment for hyperlipidemia and hypercholesterolemia. KLF2 transcript was observed elevated in HUVECs treated with various statin family members. When these cells were later

treated with KLF2 siRNA, the typical upregulation of thrombomodulin (THBD), eNOS, and integrin β4 was abolished. Simultaneously, monocyte chemotactic protein 1 (MCP-1) downregulation, a potential cause of the anti-inflammatory effect of statins, was also lost (Parmar, 2005). The differential expression patterns could identify these genes as potential KLF2 targets, implicating a role for KLF2 as an anti-atherosclerotic gene. Similarly, KLF2 overpression in HUVECs upregulated eNOS expression while inhibiting expression of vascular cell adhesion molecule-1 and endothelial adhesion molecule E-selectin in response to various pro-inflammatory cytokines (SenBanerjee, 2004). Again, these findings point to KLF2 as a pro-inflammatory regulator. In the immune system, KLF2 knockdown and overexpression experiments *in vitro* demonstrated a repressive role in monocyte secretion of cytokines, in phagocytic capacity, and in carrageenan-induced inflammation *in vivo* (Das, 2006). Carrageenans are a family of sulphated polysacharrides extracted from seaweed, found to elicit a predictable inflammatory response when injected into mouse models.

From the evidence discussed, KLF2 has a diverse set of cardiovascular functions in both development and the adult mouse. Additional work has shown that KLF2 appears to negatively regulate the differentiation of pre-adipocytes to adipocytes *in vitro* (Wu, 2005). Surprisingly, while KLF2 was first identified based on its expression in the lungs, few studies have been devoted to elucidating its role in this organ; although chimeric KLF2-/- mice that survived past birth exhibited lung abnormalities (Wani, 1999). Instead, scientists have opted to focus their research on its role in erythropoiesis, development, and the vascular system. Lastly, KLF2 has been shown to have a role in immune function, being required for T cell quiescence maintenance in peripheral blood (Kuo, 1997; Haaland, 2004).

Krüppel-Like Factor 4

KLF4 is located on mouse chromosome 4. KLF4 transcripts are highly expressed in the gut, lungs, skin, and testis of the adult mouse (Sheilds, 1996; Segre, 1999), and can also be found in mesenchymal cells, forelimb buds, and primitive eye during development (Ehlermann, 2003). KLF4 is required for the barrier function of the skin, evidenced by knockout models. (Segre, 1999)

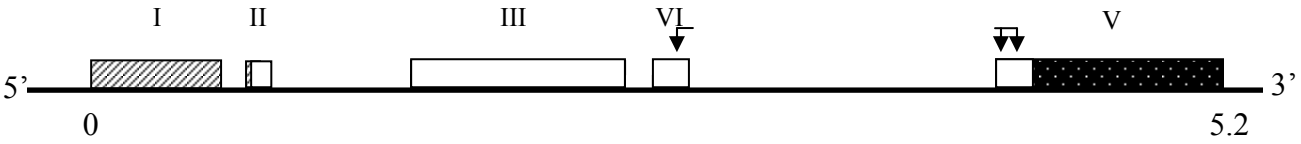

Figure 5: Structure of KLF4 gene on mouse chromosome 4. The boxes indicate exons, numbered with roman numerals, clear boxes indicate translated codons, the dashed boxes indicates the 5'UTR, the spotted box indicates the 3'UTR. The bracketed arrows indicate the three C2/H2 zinc fingers. Scale is given in kilobase pairs.

KLF4 KO Mice were produced using a targeting vector containing a PGK promoter-driven neomycin gene to delete 2.8 kb, including exons 2, 3, and a portion of exon 1 through homologous recombination in ES cells (Segre, 1999). KLF4 KO mice die soon after birth due to failure of the skin-barrier function. No vascular phenotype has been reported in these mice during development (Segre, 1999).

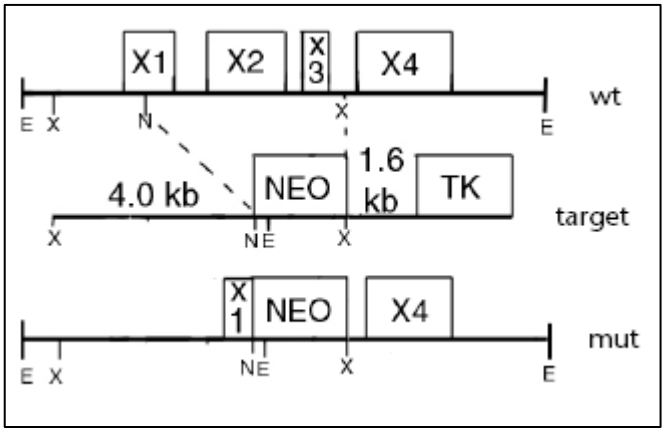

Figure 6: Disruption of KLF4 gene. KLF4 wild-type gene is recombined with PGK-driven neomycine cassette, generating KLF4 knockout allele. E, EcoRI; N, NotI; X, XbaI (Segre, 1999).

In the mouse embryo, KLF4 RNA is first detected at E4.5 in extraembryonic tissues, and in mesenchyme at E10.5, followed by epithelium (Ehlermann, 2003), and has been detected in mouse primitive erythrocytes (Gabriel Eades, unpublished data). KLF4 RNA has been shown to be expressed in endothelial cells of adult C57/Bl6 mice, in both arteries and veins (Hamik, 2007) by northern blot and in-situ hybridization. KLF4 RNA was shown to be highly induced by laminar shear stress in HUVEC culture, mirroring the upregulation of other thromboprotective factors such as eNOS and THBD (Gimbrone, 2000; Topper, 1996). Hamik also showed that KLF4 regulates the eNOS and THBD genes in COS7 cells using a luciferase reporter assay. This was interesting, given that these two genes were also upregulated during KLF2 overexpression *in vitro*. A recent study demonstrated that in cultured VSMCs over-expressing KLF4, KLF4 binds promoter/enhancer regions of the gene for the cell cycle inhibitor, p21, leading to reduced cellular proliferation after injury. In the same study, KLF4 was conditionally knocked out in a temporal manner using tamoxifen and Cre-ERt system. Here, the Cre enzyme was fused with the human estrogen receptor (ERt), which penetrates the nucleus when exposed to tamoxifen, a ERt antagonist, leading to Cre-mediated KLF4 gene excision. In this manner, Owens was able to study adult KLF4-/- mice by bypassing post-natal lethality. The adult KLF4 conditional KO mice generated through this method displayed thickened arterial intima following injury consistent with the overexpression data (Yoshida, 2008). KLF4 plays roles in phenotypic switching, or cells switching between two cell types, and proliferation of VSMCs (Zheng, 2010).

KLF4 mRNA can be induced in rat primary VSMC using TGFβ (transforming growth factor beta) family proteins TGFβ1, BMP (bone morphogenetic protein) 2, BMP4, BMP6, and BMP7. These growth factors orchestrate tissue architectural growth throughout the body (King, 2003). KLF4 abolishes smooth muscle expression of genes co-induced by myocardin & serum

response factor (Liu, 2005). These results suggest that KLF4 expression may be upregulated by pro-growth proteins, as a means to modulate development of the organism. When KLF4-/- is deleted in the gut epithelia of Foxa3-Cdx2 mice through a Cre-system, these mice showed increased proliferation and altered differentiation of gut epithelia (Katz, 2005). This result is interesting given the altered differentiation of the skin seen in the post-natal KLF4 KO mice, as this phenotype led to embryonic lethality (Segre, 1999).

Extensive research on the role of KLF4 in VSMC has lead to discoveries of its complicated role in cancer. KLF4 has been shown to mediate the actions of p53 on the p21WAF1/Cip1 promoter. The downstream effectors of KLF4 can both halt cell cycle progression as a result of DNA damage and advance it (Zhang, 2000; Yoon, 2003; Rowland, 2005). As such, KLF4 appears to have both oncogenic and anti-oncogenic roles in mediating the cell cycle. KLF4 expression is nearly absent in the cells of intestinal and diffuse-type gastric cancers compared to normal tissue, indicating that it may have roles in either angiogenesis or cell cycle regulation (Katz, 2005).

Recently, it was shown in HEK293T (an embryonic kidney cell line) and HCT116 (a colonic epithelial cell line) culture that KLF4 inhibits p300/CBP-mediated β-catenin aceylation and Wnt **(**Wingless and Int genes**)** target gene histone acetylation, indicating that it may play a larger epigenetic role (Evans, 2010). KLF4 RNA is highly expressed in mouse cornea (Norman, 2004), and when the gene is ablated using a conditional knockout in the eye, resulted in corneal epithelial fragility without obvious loss of cell junctions, leading to stromal edema and loss of goblet cells in the conjunctiva (Swamynathan, 2006). Interestingly, these mice also had more bulbous endothelial cells in the cornea. KLF4 regulates monocyte differentiation in overexpression studies in HL-60 cells, generating mature monocytes, while knockdown of KLF4

prevents maturation (Feinberg, 2007). Conversely, KLF2 inhibits pro-inflamatory activation of monocytes *in vivo*.

Ablation of KLF2 & KLF4

EKLF, KLF2, and KLF4 are about 90% similar in the zinc finger domain at the amino acid level (reviewed by Philipsen, 1999; Bieker, 2001). Having demonstrated that EKLF and KLF2 compensate for each other in embryonic globin production and that the EKLF/KLF2 double KO embryos die sooner in development than either single KO, it was hypothesized that KLF2 and KLF4 might also play overlapping roles in development.

This study aims to observe the consequences of combined KLF2 and KLF4 ablation using previously established KLF2 and KLF4 knockout mouse models to generate a combined KLF2/KLF4 double knockout (DKO) mouse. Recognizing that KLF2 KO mice die *in utero* by approximately day 12.5 post-coitus (E12.5), examination of embryos prior to this stage is required to elucidate any developmental roles prior to the onset of death. Preliminary data indicated that KLF2-/- KLF4-/- mice die by E10.5 and can exhibit cranial bleeding (Figure 7H). All KLF2/KLF4 DKO embryo appeared dead at E10.5 without any heartbeat (n=3). Of these, one embryo showed gross hemorrhaging in the head (Figure 7H). For the remaining genotypes at E10.5, three KLF2-/-KLF4+/- embryos (n=7) and two KLF2+/-KLF4-/- embryos (n=12) exhibited gross cranial bleeding (represented in Figures 7G, 7D, respectively). All other genotypes appeared grossly normally at this age (Figure 7).

When these mice were embedded and sectioned, E10.5 KLF2/KLF4 DKO tissue was necrotic with poor morphology. As such, E10.5 KLF2-/-KLF4+/- embryos (Figure 8A-C), also found to have cranial bleeding, were previously sectioned and seen with cranial hematoma and

endothelial disruption of the primary head vein (PHV or PH). This phenotype was not seen in KLF2-/- embryos grossly, or in transverse section (Figure 8D-F).

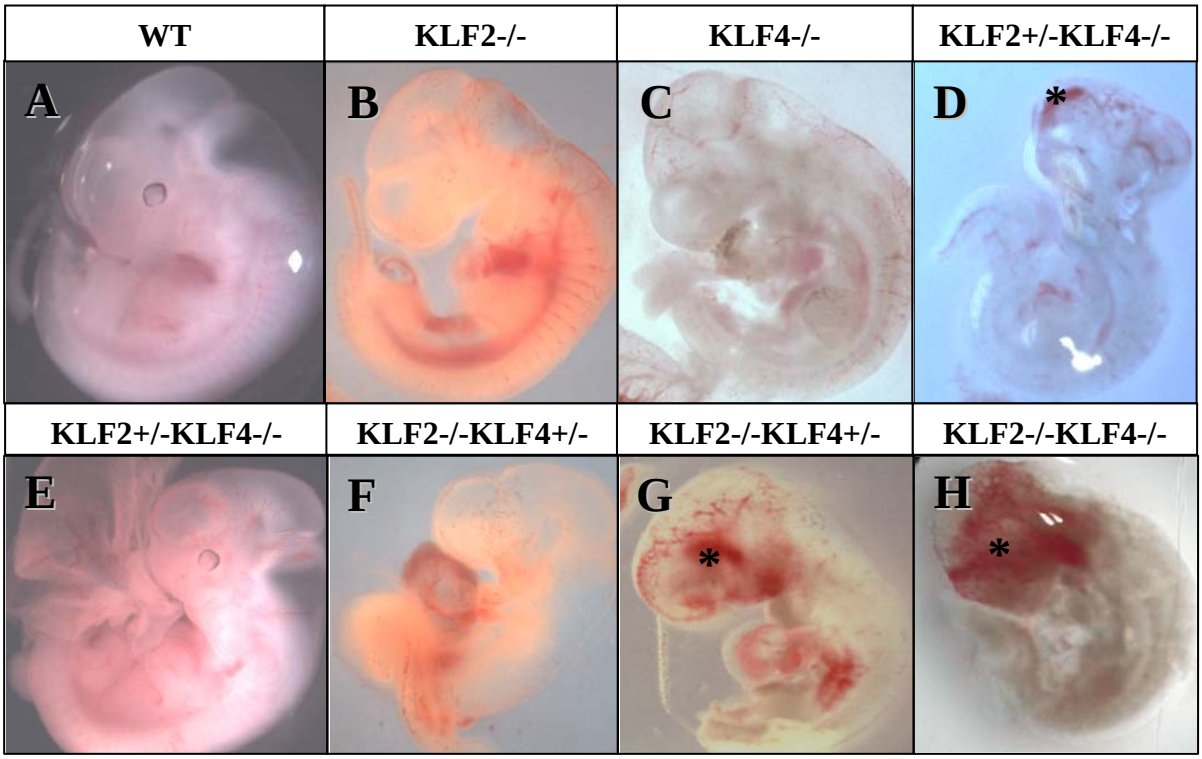

Figure 7: Whole mounts of KLF2 KLF4 knockout mice at E10.5. KLF2-/-KLF4-/- (H) has severe cranial bleed, while KLF2+/-KLF4-/- (D) and KLF2-/-KLF4-/- (G) also has cranial bleed of less severity. Images are courtesy of Sean Fox and Megan Smith (unpublished data). Asterisks identify cranial bleeds. Images are magnified ~30X.

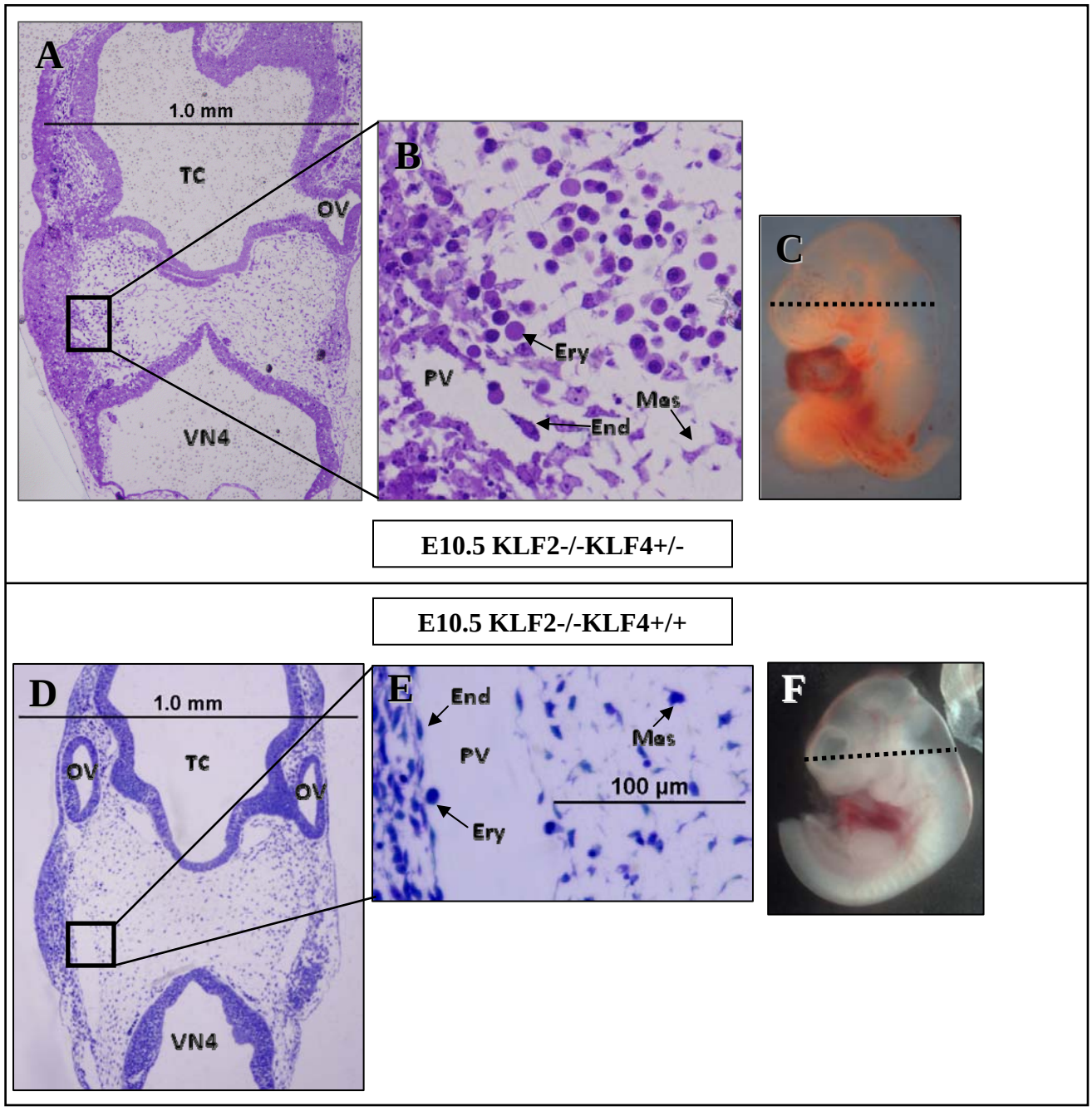

Figure 8: Transverse sections of KLF2/KLF4 knockout mice at E10.5. Sections are courtesy of Sean Fox and Megan Smith (unpublished data). E10.5 KLF2-/-KLF4+/- embryo (A-C) has discontinuous endothelial layer with escaping erythrocytes compared to E10.5 KLF2-/- (D-F) embryo. Asterisks identify cranial bleeds. TC, telencephalic vesicle; VN4, fourth ventricle; OV, optic vesicle; PV, primary head vein; Ery, erythrocyte; End, endothelial cell; Mes, mesenchymal cell. Dashed lines indicate approximate level of section. (A, D) 4X, (E) 10X, (B) 20.

Relevance

Understanding the roles of the KLFs in cardiovascular development may prove valuable in understanding and treating congenital heart defects (CHD); these illnesses, currently affect 4 - 50/1,000 live births, depending on the clinical study (Hoffman, 2002). Even more pressing, of children born with CHDs, only approximately 85% reach adulthood as of 2001 (Warnes), indicating that research into the molecular mechanisms involved in CHDs is urgently needed. Recently, KLF2 was shown to be vital in forming the atrioventricular (AV) cushions in the mouse embryonic heart, with E9.5 KLF2-/- having multiple disorganized layers in the developing AV valves with reduced glycosaminoglycans at E10.5 in the cardiac jelly (Chiplunkar, unpublished data).

As both KLF2 and KLF4 are induced via shear stress, and KLF2 has an inflammatory function, KLF2 and KLF4 may have possible roles in atherosclerosis, the primary cause of cardiovascular disease, the leading cause of death in the United States (Thom, T. *et al.*, 2006).

Studying vascular development may ultimately provide the tools for most efficaciously managing cancer, given the necessary vascular signals needed for tumor blood supply, leading to outgrowth and spread. Additionally, tumor and endothelial cell reciprocal signaling have been demonstrated as required for progression towards malignancy (Orr, 2000). It has been postulated that physicians and researchers may one day design therapies that utilize the same malfunctioning vascular mechanisms for effective drug delivery (Pasqualini, 2002).

Aims of study

This study examines the hypothesis that KLF2 and KLF4 genes regulate a shared set of downstream effectors that have a function in vascular maintenance in or around the primary head

vein in developing mice. Foremost, this study will further characterize the defects that lead to problems with cardiovascular development in KLF2-/-KLF4-/- mouse tissue. Since many vascular development genes, when deleted, give rise to global vascular deficits, whole embryos were examined grossly for changes in the vasculature at E9.5. Sections of E9.5 KLF2-/-KLF4-/- mice were examined for vascular abnormalities and other novel findings, followed up by ultrastructural analysis. As seen through the altered expression of KLF2 and KLF4 in knockout, knockdown, or overexpression studies, the high possibility arises that KLF2 and KLF4 may regulate a set of overlapping downstream effectors. This is even more likely as they are both upregulated in HUVEC culture in response to laminar flow (i.e. shear stress). A set of candidate genes will be tested with qRT-PCR on WT, KLF2-/-, KLF4-/-, and KLF2-/-KLF4-/- to measure possible differential expression patterns at specific loci. Testing the DKO is especially important, as changes in expression following the ablation of one gene may be masked by the functional compensation of the other.

Chapter 2: Materials and Methods

Generation of mice

KLF2+/- mice were generated by and obtained from Dr. Jerry Lingrel **(**Wani, 1998**)**. KLF4+/- mice were generated by and obtained from Dr. Julie Segre **(**Segre, 1999**)**. KLF2 and KLF4 are located on mouse chromosomes 8 and 4, respectively, and therefore segregate independently in meiosis. KLF2+/- and KLF4+/- mice were bred to generate KLF2+/-KLF4+/- double heterozygous mice. KLF2+/-KLF4+/- males were mated with wild type (WT) FVB/N females to produce additional KLF2+/-KLF4+/- mice to preserve the line. Once KLF2+/-KLF4+/- females were approximately 6 weeks old and weighed at least 23.0 g, they were bred with KLF2+/-KLF4+/- males. This mating generated homozygous KLF2-/-KLF4-/- double knockout (DKO) embryos and embryos to serve as controls: WT, KLF2+/-KLF4+/-, KLF2-/-, KLF4-/-, KLF2+/-KLF4-/, KLF2-/-KLF4 +/-. Peanuts were given to females to encourage weight gain and support pregnancy. Every morning during these timed matings, females were checked for vaginal plugs, a coagulation of male semen, signifying that coitus had recently occurred, establishing the time of gestation as day 0.5 post-coitus (dpc). At this time, the female mouse was separated and dissected at 9.5 or 10.5 dpc, corresponding to E9.5 or E10.5 (embryonic day) embryos. Somite counts were used as developmental markers to confirm that litters were of the same approximate developmental age (E9.5 = 21-29 somites, E10.5 = 35-39 somites).

Genotyping

Polymerase Chain Reaction (PCR) was utilized to determine the genotype of dissected embryonic specimens and mice. Ear punches or tail clips were incubated at 60°C for

approximately 12 hours in 70 µL digestion buffer (50mM KCl, 10mM Tris HCl [pH 8.5], 40mM $MgCl_2$, 0.45% Nonidet P40 lysis buffer, and 0.45% Polysorbate 20) containing an additional 7 µL of 10µg/mL Proteinase K, a serine protease. Upon completion, the Proteinase K was deactivated through a 10 minute heating cycle at 95°C, cooled to 4°C and zip-spun for ten seconds in an Eppendorf 5415C micocentrifuge. The sample was again heated, cooled, and zip spun prior to PCR. A stock solution of PCR grand mix (GM) was prepared with 10X PCR buffer (200 mM Tris-HCl [pH 8.4], 500 mM KCl), 0.2 mM dNTPs, 1.5 mM $MgCl_2$, 0.5 µM forward KO primer, 0.5 µM reverse KO primer, 0.5 µM forward WT primer, 0.5 µM reverse WT primer (Table 1). Primers were designed based on the known sequence of wild-type (WT) and knockout (KO) alleles at KLF2 and KLF4 loci. Right before initiating PCR, master mix (MM) was prepared with PCR GM, *Taq* DNA Polymerase (0.04 U/µL), RNase A (0.07mg/µL), and molecular grade water. 22-24 µL MM and 1-3 µL DNA digestion extract were placed in eight-strip PCR tubes for a total reaction volume of 25 µL. All reactions were performed in duplicate, using previously genotyped cellular extracts as KLF2 and KLF4 positive control samples, and molecular grade water as a negative control. The PCR consisted of an initial denaturation step at 94°C, followed by 35 cycles of 40 sec at 94°C, 45 sec at 58°C, and 75 sec at 72°C. The reaction was terminated by a final extension for 5 min at 75°C. A 2% agarose gel was prepared, consisting of 100 mL 1X TAE buffer (2 M Tris, 10 mM Glacial Acetic Acid, 10 mM EDTA [pH 8.0], dH_2O) and 2.0 g Seakem LE agarose, and 5 µL 10% ethidium bromide. The TAE and agarose were combined in an Erlenmeyer flask and heated in a Sharp Electronics microwave oven for approximately four minutes at which time the solution turned uniformly transparent. When boiling had eased, the ethidium bromide was added, and the solution was poured into a gel casting tray. Twenty-lane gel combs were inserted (either before or immediately after gel

pouring) and the gel was set for approximately half an hour to fully solidify. At that time, the gel basin was filled with 1X TAE, submerging the gel. 10 µL of each PCR product was mixed with 1 µL Ambion Gel Loading Buffer II and then loaded into the respective well. Additionally, 0.175 µg of 100 bp ladder, along with the aforementioned positive and negative controls were loaded into each row. Electrophoresis was performed between 50 – 90 min at 95 V until the products resolved, checked periodically by Entela UVG Mineralight at 254 nm ultraviolet light.

	Forward Primer (5' to 3')	Reverse Primer (5' to 3')	Amplicon Size (bp)
KLF2 – WT	TTGCCGTCCTTTGCCACTTTCG	TTGTTTAGGTCCTCATCCGTGCCG	380
KLF2 - KO	CGGTCTCTTGTAGCCAAAGGG	CAAAGAACGGAGCCGGTTGG	313
KLF4 – WT	CAGCTTCATCCTCGTCTTCC	AGACGCCTTCAGCACAAACT	320
KLF4 – KO	GCCCAGTCATAGCCGAATAG	GACCAGAATAGAGTCAAGGGTTAGG	270

Table 1: KLF2 and KLF4 PCR primer sets: KLF2/KLF4 WT and KO primer sets to amplify unique gene regions, establishing the genotype of mouse pups and dissected embryos. The amplicon size, established by the PCR product migration on an agraose gel, was the diagnostic tool in determining the mouse genotype.

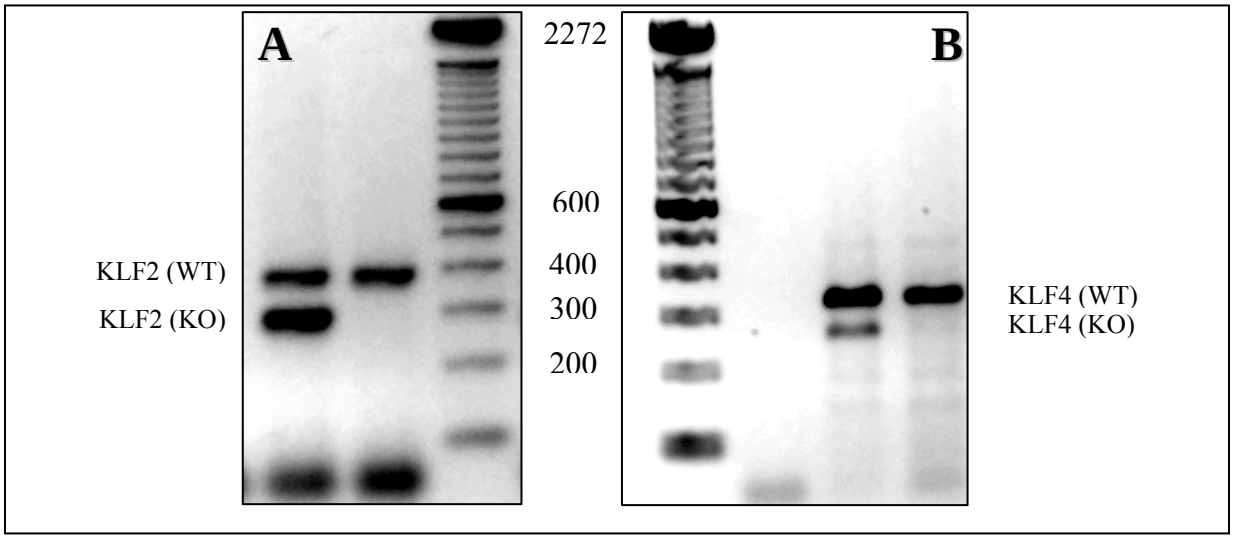

Figure 9: KLF2 and KLF4 gel electrophoresis: Migration of amplified KLF2 (A) and amplified KLF4 (B) genes on a 2% agarose gel. The blank lane in figure 9B represents a negative control with only a visible primer band. Size given is in base pairs.

Chi-Square Analysis

To establish the time of death, embryos were dissected at E9.5 and E10.5. Observed embryo genotypes were listed against expected embryo genotypes, based on Mendelian genetics. Again, the KLF2 and KLF4 genes are located on chromosomes 8 and 4 and therefore segregate independently during meiosis. Comparing the expected genotypes to the observed genotypes, a Pearson's chi-squared analysis was performed to test for fit of the expected distribution.

Microdissection of E9.5 embryo and yolk sac

When pregnant mice reached E9.5, or nine days following vaginal plug visualization, they were relocated to a dissection room and exposed to inhalation anesthesia, 1 mL isoflurane, sprayed on a 4x4 gauze pad in a 1 L closed container for approximately 30 seconds. The pregnant mice were then quickly removed and injected with 2.5% Avertin (10 g tribromoethanol, 10 mL tert-amyl alcohol) at approximately 0.015 mL/g body mass. A physical pinch to the lower limb confirmed effective sedation, followed by prompt mechanical cervical dislocation. Embryos were excised from their implant sites and dissected in 1X Phosphate Buffered Saline (PBS), contained in 30 mm Petri dishes with watchmaker forceps and surgical scissors, magnified (6.7X – 40.5X) with an Olympus SZ2-ILST dissection microscope. Following removal of the maternal decidua and embryonic chorion, the yolk sac and embryo were detached and photographed with an Olympus Q-Color 3 camera using QCapture 2.81.0 imaging software after aligning the embryonic spine with a metric ruler. Developmental age was confirmed via crown-rump length and somite counts (21-29). An approximately 1 mm section of tail was removed and genotyped via the procedure outlined earlier. The remaining yolk sac and embryo were transferred to tooled neck glass vials or cryotubes and either (1) quick-frozen in liquid

nitrogen for analysis via quantitative reverse transcriptase polymerase chain reaction (qRT-PCR), (2) placed in 4% paraformaldehyde (PFA) fixative for immunohistochemistry or in-situ hybridization, or (3) placed in 2% PFA/2.5% glutaraldehyde fixative for plastic-sectioned light microscopy and electron microscopy. Tissue quick-frozen in liquid nitrogen was transferred to a -80 °C. freezer when the dissection was complete, and stored there until processing.

Tissue preparation for light and electron microscopy

Fixed embryo and yolk sac were removed from 2% PFA/2.5% glutaraldehyde after 24 hours and washed three times for five minutes each in Millonig's phosphate buffer (109 mM NaOH, 136 mM sodium biphosphate), and then osmificated at room temperature for 40 – 60 min in 1% osmium tetroxide. The tissues were serially-dehydrated in 30%, 40%, 50%, 60%, and 70% ethanol for 5 minutes each and 80%, 95%, 100%, 100% ethanol for 10 minutes each. Afterwards, the specimen were cleared in a 1:1 mixture of ethanol and propylene oxide for 10 minutes, and 100% propylene oxide for 10 minutes, twice. The samples were held overnight in a 1:1 mixture of propylene oxide and eponate 12 resin, and transferred the next day to 100% eponate 12 resin and set for several hours. The specimens were carefully removed with a toothpick and placed in a cutting-block mold with eponate 12 resin, incubated in an oven overnight at 55 °C. The plastic blocks were removed from their molds and trimmed to size.

Light & electron microscopy

Plastic embedded specimen were cut in transverse section (cross-section) at 2 μm and 6 μm thick for yolk sac and embryo, respectively, on a Sorvall JB4 Microtome. Sections were carefully placed on a Fisher Scientific Superfrost Plus microscopy slides, spotted with water to

encourage section adhesion. Water was slowly vaporized on a hot plate before staining with solution composed of 1% sodium borate, 1% azure II, 1% toluidine, and 1% methylene. Stained sections were photographed with an Olympus DP71 digital camera, mounted to an Olympus BX41 compound microscope, visualized with Olympus DP Controller 3.2.1.276 imaging software.

For transmission electron microcopy (TEM), thin sections were cut at 100 nm on a LKB 2128 Ultratome, followed by staining with 5% uranyl acetate and Reynold's lead citrate. Images were taken using a JEOL JEM-1230 TEM and Gatan Ultrascan 4000 digital camera at 1,000 – 8,000X.

Mesenchymal cell counts at the level of the optic vesicle were made using the sections examined by light microscopy. These cell counts were confined to a standardized area (1) immediately medial to the primary head vein, or (2) immediately near the midline. Counting criteria for cells were a visible nucleus, and width at least ¼ the length.

Whole-mount imunohistochemistry

KLF2+/-KLF4+/- female mice were mated with KLF2+/-KLF4+/- males to generate E9.5 KLF2-/-KLF4-/- embryos. These embryos were fixed overnight in 4% PFA in PBS, washed with PBS four times, treated through serial ethanol dehydration: 30%, 50%, 70%, 95%, 100%, 100%, 100% and stored at -20°C. Samples were rehydrated stepwise to PBS with 0.1% Polysorbate 20 (PBST): 30%, 50%, 70%, 95%, 100%, and 100%. The embryos were washed four times in PBST for 15 min each, followed by incubation in 0.5% hydrogen peroxide, 0.5% serum in PBST for 30 min at room temperature. The samples were placed in antibody blocking solution (10% goat serum in PBST) for 2 hr at room temperature. The samples were incubated overnight at 4°C

in primary antibody, PECAM (1:200) in antibody blocking solution. The next day, the embryos were washed four times for 30 min in antibody blocking solution. The embryos were placed in secondary antibody, biotinylated Anti-Rat IgG (1:500) for 2 hr at room temperature. The samples were again washed in PBST as before, and incubated in pre-diluted BD Pharmingen Streptavidin-Horseradish Peroxidase (Sav-HRP) for 1 hr at room temperature. After washing four times for 30 min in PBST, the embryos were incubated in BD Pharmingen 3,3'diaminobenzidine (DAB) chromogen in H_2O_2 buffer for approximately 5 min. After washing with PBST to remove DAB, the embryos were fixed overnight in 4% PFA in PBS at 4°C. The next day, the embryos were washed in PBS, dehydrated in methanol and rehydrated in PBS. The samples were cleared in 50% glycerol/PBS for 1 hr. The samples were mounted on slides in 80% glycerol. Coverslips were placed on the slides and digital pictures were taken with an Olympus DP71 digital camera, mounted to an Olympus BX41 compound microscope, visualized with Olympus DP Controller 3.2.1.276 imaging software.

In-situ hybridization of E10.5 embryo for KLF2 and KLF4

A frozen aliquot of *E. coli* containing a pCMV-SPORT6 plasmid with a 2.2kbp KLF4 cDNA insert was purchased from ThermoScientific OpenBiosystems (MMM1013-64603). Ampicillin agar plates were prepared by combining 5.0 g tryptone, 2.5 g yeast extract, 5.0g NaCl, 7.5 g agar, brought to a volume of 500 mL with dH_2O. These ingredients were autoclaved and treated with ampicillin for a final concentration of 100 µg/mL. The culture was streaked on an ampicillin agar plate with an inoculating loop and incubated at 37 °C overnight. The next day, individual colonies were isolated by touching them with a sterile pipette tip and submerging them in 1 mL of autoclaved yt-amp broth (16 g tryptone, 10 g yeast extract, 5 g NaCl, 1 mg/mL

ampicillin, bringing the total volume to 1 L with dH_2O). This small culture was incubated on a rotator plate for approximately 12 hours before transferring the culture to a 1 L Erlenmeyer flask with 1 L autoclaved yt-amp broth. The flask was left on the rotater at 37 °C for approximately 16 hours. 400 mL of broth was deposited into eight 50 mL Corning Centrifuge Tubes and spun down on a Sorvall RT7 Plus centrifuge at 4000 rpm for 10 min. Using the Promega PureYield™ Plasmid Miniprep System, the pelleted cells were resuspended in 3 mL of Resuspension Solution and combined into two 50 mL centrifuge tubes. 12 mL of Cell Lysis Solution was added followed by inversion. After 3 minutes, 20 mL of Neutralization Solution was added, followed by inversion. The lysate was centrifuged at 4000 rpm for 15 min. A column stack, composed of a clearing column and binding column from the Promega pack were stacked onto a hose connected to a Büchner flask, hooked up to a vacuum. The supernatant collected from the 50 mL centrifuge tubes was slowly poured into the clearing column with vacuum being applied. Once all the liquid had been filtered, 5.0 mL of Endotoxin Removal Wash was added, and when completely filtered, an additional 20 mL of Column Wash Solution was added. The column was dried by vacuum for 1 min, and the binding column was removed. The clearing column was soaked with 600 µL Nuclease-Free Water and dropped into a new 50 mL centrifuge tube, which was then spun down at 4000 rpm. The water at the bottom of the tube containing the DNA was collected, and treated with 1 µL of 10mg/mL RNAse A. The nuclease-treated sample was analyzed with Thermo Scientific NanoDrop™ ND-1000 Spectrophotometer at 230 nm, 260 nm, and 280 nm to determine nucleic acid concentration, DNA purity, and organic contamination.

The collected DNA sample was tested for plasmid purity using restriction enzyme digestion. On a 1% agarose gel, the following digests were run: (1) undigested plasmid; (2) plasmid and HindIII; (3) plasmid and EcoRI; (4) plasmid, HindIII, and EcoRI. 0.175 µg of 1kbp

ladder was loaded to identify band fragment lengths and confirm plasmid isolation. 10 µL of 100 ng/µL undigested plasmid was submitted to the VCU DNA Core Facilities for sequencing to determine orientation of inserted KLF4 cDNA fragment.

As the possibility arose of cross-reactivity between KLFs using a probe containing the zinc finger region, new probe templates were engineered using the purified pCMV-SPORT6 vector. 10 ng of purified pCMV-SPORT6 was added to a PCR reaction mixture with solutions and concentrations identical to the KLF2/KLF4 PCR in a previous section. The primers utilized included sequences with T7 and T3 promoters bracketing KLF4 cDNA sequences outside of the zinc finger region. The actual sequences are listed in Table 2, and ultimately the KLF2 probes (T7-K2-439 and T3-K2-439) yielded a successful hybridization. The PCR thermocycling program consisted of an initial denaturation step at 94°C, followed by 35 cycles of 40 sec at 94°C, 45 sec at 58°C, and 75 sec at 72°C. The reaction was terminated by a final extension for 5 min at 75°C.

The K2-ZnF1 plasmid available in the laboratory contains KLF2 cDNA (276-790, NM_008452.2) cloned into pBSK(-) and excludes the zinc finger region. Generation of PCR product from the GC-rich coding region of K2-ZnF1 KLF2 cDNA failed with the standardized KLF thermocylcing program. A Finnzymes-brand Phire Hot Start DNA Polymerase kit was used to generate product with a high temperature thermocylcing program. 1 ng K2ZnF1 was combined with 0.4 uL Hot Start Polymerase, 4 µL reaction buffer, 0.4 µL 10 mM dNTPs, 1 µL 10 uM forward primer, 1 µL 10 µM reverse primer, brought to 20 µL with RNAse-free water. The thermocycling program consisted of an initial denaturation step at 98°C, followed by 35 cycles of 5 sec at 98°C, 5 sec at 80°C, 20 sec at 72°C. The reaction finished with 72°C for 1

min. The reaction solutions were treated with 1 µL Ambion SUPERase-In (20U/µL) to deactivate RNase.

ID	Primer Sequence	Tm (°C)	Amplicon Size (bp)
T7-K4-506	TAATACGACTCACTATAGGGGGTTTTGGTTTGAGGTTT	67.9	546
T3-K4-506	ATTAACCCTCACTAAAGGGAAAGACGAGGATGAAGCT	69.1	
T7-K4-200	TAATACGACTCACTATAGGGATAAGGCCTGGGTGGGC	72.4	298
T3-K4-200	ATTAACCCTCACTAAAGGGACAATCCCATGGAGAGGATGAA	70.7	
T7-K2-439	TAATACGACTCACTATAGGGAACAGAGCTGCTGCGCCC	73.3	439
T3-K2-439	ATTAACCCTCACTAAAGGGAGCGTCCTCGAAAAGACCGA	72.1	

Table 2: Riboprobe synthesis DNA template primers for PCR. This table displays the primers used to generate the PCR product then used as a template for a reverse transcription in-situ probe synthesis. T7 RNA polymerase generated sense probe templates, and T3 RNA polymerase generated antisense probe templates.

The PCR Products were purified using a Qiagen QIAquick PCR Purification Kit. To the PCR reaction solution, 5 volumes of Buffer PB was added (100 µL). The contents of several tubes were combined and poured into QIAquick column inside a 2 mL collection tube. The column was spun in a table microcentrifuge at 14,000 rpm for 1 min. After discarding the flow-through, the column was washed with 0.75 mL Buffer PE and again centrifuged for 1 min. at 14,000 rpm. The flow-through was discarded, and the column was centrifuge for an additional 2 min. to remove any traces of remaining ethanol still on the column. The column was then placed in a clean 1.5 mL microcentrifuge collection tube. To the center of the colum membrane, a volume of 50 µL ultrapure DEPC (diethyl pyrocarbonate)-treated water was deposited and allowed to diffuse for 1 min. The column was centrifuged for 2 min. at 14,000 rpm. 1 µL of purified PCR product was then analyzed on a NanoDrop™ ND-1000 Spectrophotometer and 1 µL run on a 2% agarose gel to check product identity, concentration, and purity.

The RNA riboprobes were synthesized using an Ambion MAXIscript in vitro transcription kit. Here, 1 µg DNA template (either purified PCR product or digested plasmid), 2 µL 10X transcription buffer, 2 µL 10X Roche DIG RNA Labeling Mix (10 mM APT, 10 mM

CPT, 10 mM GPT, 6.5 mM UPT, 3.5 mM DIG-11-UTP), and 2 µL T3 or T7 enzyme mix were added to the reaction tubes. The reaction was brought to 20 µL volume with ultrapure (DEPC-treated) water and incubated at 37°C for 1 hr. 1 µL TURBO DNase (20U/µL) was added and the mixture was incubated at 37°C for an additional 15 min. The reaction mixture was brought to 50 µL with ultrapure (DEPC-treated) water and 9 µL 3M NaOAc was added. The solution was vortexed, and three volumes of 100% ethanol (180 µL) were added, and 1 uL 5 mg/mL glycogen was added to encourage RNA precipitation. The solution was stored at -80°C for 1 hr. After spinning for 15 min. at 16,000 rpm in a 4°C refrigerated microcentrifuge, the supernatant was removed, and the pellet was washed with 180 µL 70% ethanol. The tube was re-centrifuged for 10 min., and the supernatant was removed. The pellet air dried for about 2 min. and was resuspended in 50 µL ultrapure (DEPC-treated) water. 1 µL probe was run on a 2% agarose gel to confirm expected probe length, and 1 µL analyzed on a NanoDrop™ ND-1000 Spectrophotometer to determine probe concentration and purity. The RNA probe lengths expected were the same as the product length for the PCR product template.

E10.5 FVB/N WT embryos were dissected as outlined above for KLF2/KLF4 DKOs. E10.5 embryos were selected as they were larger and hence, more resistant to tissue processing. The embryos were fixed overnight in 4% PFA that was generated using DEPC-treated ultrapure water. During the tissue processing and hybridization procedure, all generated reagents were made using DEPC-treated water. After fixation, the embryos were washed for 1 min. with PBS and then for 30 min., four times. The tissue was serial dehydrated: 30% ethanol for 2 hours, 50% ethanol for 2 hours, 70% ethanol for 4 hours, 95% ethanol overnight, 100% ethanol for 1 hour, 100% ethanol for 1 hour. The specimens were stored at -20 °C prior to processing. On the day of the hybridization, the samples were washed with 100% ethanol three times at room temperate.

The embryos were cleared twice in xylenes for 30 min. and submerged in melted paraffin (~ 60 °C) for 40 min., three times. The tissue was embedded in paraffin after placement in a stainless steel mold and stood upright on its head as the wax hardened. A Simport Micromesh Biopsy Embedding Cassette was placed on top of the hardening wax and would later serve as an anchor in the paraffin-use microtome. The paraffin blocks were stored at 4 °C overnight and sectioned to 6 μm on a Shandon AS325 microtome. The tissue sections were placed in a water bath filled with DEPC-treated water, scooped up onto Fisher Scientific Superfrost Plus microscopy, and air dried. The slides were stored at room temperature and used within a week.

On the day of the hybridization, the slides were warmed at 60 °C for 1 hr in a Barnstead Lab-Line MaxQ 4000 Incubator. Deparaffinization took place by incubating the slides for 20 min. in 60 °C xylene, twice. The slides were rehydrated in 100% ethanol for 2 min. twice and in 95% ethanol for 2 min. once. They were then washed with 0.9% NaCl for 5 min. and incubated in 0.2 M HCl for 15 min. The HCl was removed with three 1 min. 1X PBS washes, followed by incubation with a proteinase K solution (20 μg/mL proteinase K, 50 mM Tris [pH 7.6], 5 mM EDTA) for 8 min. A solution of 0.4% glycine in PBS was used twice for 2 min. each to halt the tissue digestion, and the slides were washed with 0.9% NaCl for 2 minutes, twice. The slides were treated with 0.1 M triethanolamine with an addition of 1 mL acetic anhydride for 10 min. The tissue was washed with DEPC-treated water twice and dehydrated through 95%, 100%, and 100% ethanol for one min. each. After air-drying, the slides were laid flat and spotted with 60 μL 1:25 RNA probe diluted in hybridization mix (50% Sigma 2X Prehybridization Solution, 0.25% Roche Baker's Yeast tRNA, 0.08% heparin, in super-grade formamide). The probe was evenly spread by carefully affixing a glass coverslip. The slides were left to hybridize overnight in a 55 °C humidity chamber containing 50% formamide in 2X SSC (saline-sodium citrate). The

next day, the slides were placed in a bath of 60 °C 2X SSC for 15 min. The coverslips were carefully removed if still attached, and the slides were returned to the 2X SSC for an additional 30 min. The following washes then took place by submerging the slides: STE (sodium chloride tris EDTA) at 37 °C for 20 min, STE at 37 °C for 10 min., 2X SSC at 60 °C for 30 min, 0.5 SSC at 60 °C for 30 min, 0.1X SSC at 60 °C for 30 min., 0.1X SSC at room temperate for 1 min., ddH_2O at room temperate for 1 min, and ddH_2O at room temperature for 1 min. The slides were then washed with TBST (Tris-buffered saline with Tween-20) for 10 min., three times. The slides were laid out and the tissue was outlined using a Vector ImmEdge Pen, followed by an incubation in tissue blocking solution (Roche Blocking Reagent 0.2%, 10% lamb serum, in TBS, heated for 1 hour to 55 °C) for 1 hr. The tissue sections were incubated overnight at 4 °C with Roche anti-digoxigenin antibody conjugated to alkaline phosphatase (AP), diluted 1:1500 in tissue blocking solution. The next day, the sections were washed with TBST for 10 min., six times. The slides were laid out and tissue immersed in NTMT (100 mM NaCl, 100 mM Tris-HCl, 50 mM $MgCl_2$, 1% Tween 20, 2 mM levamisole) for 5 min., twice. The AP antibody was developed using a pre-mixed Roche NBT/BCIP detection solution. The slides were monitored and anti-sense and partner sense-stained tissue removed at the similar time. Typically, reactions took 30 min – 1 hr. to run to achieve desired staining intensity. The sections were washed with ddH_2O and counterstained with nuclear fast red for 10 min.

Selection of candidate genes

Based on the known roles of KLF2 and KLF4 as transcription factors, vascular development genes were selected as candidates that may be regulated by KLF2 and KLF4. These potential downstream regulatory elements were examined and ranked based on the

following criteria: (1) an established role in vascular development, (2) similar phenotype to DKOs at E9.5 when ablated, (3) high number of potential KLF2 and KLF4 binding sites, CCRCCC, conserved between mouse and humans, in the proximal promoter within 250bp upstream of the transcription start site, (4) high ratio of expression in endothelium & mesenchyme to other cell types at E9.5, (5) published evidence of regulation by KLF2 or KLF4 in another system. Genes assayed are included in Table 3.

Symbol	Name	Function	Primers	
			Forward (5' to 3')	Reverse (5' to 3')
eNOS	Endothelial Nitric Oxide Synthase	anti-inflammatory, smooth muscle relaxer	CTGCCACCTGATCCTAACTTG	CAGCCAAACACCAAAGTCATG

Table 3: KLF2 and KLF4 downstream candidate gene. The above table gives the candidate gene for KLF2 and KLF4 regulation that were assayed.

RNA extraction on whole E9.5 embryos

RNA was isolated from collected E9.5 whole embryos. RNA extraction was performed using a ToTally™ RNA kit. First, 200 µL of Denaturating Solution was added immediately to the cryotubes containing frozen tissue upon removal from a -80 °C freezer. This was especially important, because as the tissue thaws, ice crystals will tear cells, releasing RNAse into the solution, so denaturant should be present prior to melting so as to inactivate RNAse before significant RNA degradation occurs. The tissue was also promptly homogenized with a Fisher Scientific Genie2™ Vortex. Once the tissue was completely broken up, the starting volume was recorded, and 1 starting volume of Phenol:Chloroform:IAA was added to the lysate, followed by vortexing. The extract was left on ice for 5 minutes, and then centrifuged in a 1.7 mL centrifuge tube at 11,000 rpm in a Tomy MX-160 High Speed Refrigerated Microcentrifuge at 4°C for 5 min. The upper aqueous phase was transferred to a new 1.7 mL tube, being careful not to come

in contact with the interface. 1/10 volume of Sodium Acetate Solution is added. After mixing, 1 starting volume of Acid-Phenol:Chloroform was added, the tube was vortexed, and was again centrifuged at a speed of 11,000 rpm at 4 °C for 5 min. The upper phase was extracted and moved to a new 1.7 mL tube. An equal volume of isopropanol was added and mixed. The solution was stored overnight at -20 °C and centrifuged at 11,000 rpm at 4 °C for 15 min. A white pellet or smear having formed, the supernatant was discarded, and the pellet washed with 300 µL of 70% ethanol to remove residual salts. The resuspended pellet was centrifuged at 7,500 rpm at 4 °C for 10 min, and the supernatant was discarded. The tube was re-spun briefly, and the pellet was air before resuspension in 20 µL DEPC-treated water. A diluted aliquot of resuspended RNA was tested for concentration and degradation on an Agilent 2100 Bioanalyzer using an Agilent RNA 6000 Nano Kit.

Quantitative reverse transcriptase polymerase chain reaction on select KLF2/KLF4 candidate target genes

1 µg of RNA was combined with 1 µL Invitrogen DNase I, 1 µL 10X Reaction Buffer, brought to 10 µL in a microcentrifuge tube with DEPC-treated ultrapure water. This solution was incubated at room temperature for 15 min. at which time 1 µL 25 mM EDTA was added and the solution was heated for 10 min. at 65 °C. To the tubes, 4 µL 5X iScript Reaction Mix, 1 µL iScript Reverse Transcriptase, and brought to 20 µL with Nuclease-free water. This mixture was incubated in the following thermocycling program: 5 min. at 25 °C, 30 min. at 42 °C, 5 min. at 85 °C, and held at 4 °C until use.

Synthesized cDNA from various genotypes was combined with the following reagents, 12.5 µL Applied Biosystems SYBR Green, 1 µL 10mM candidate gene forward primer, 1 µL candidate gene reverse primer, brought to 25 µL total with ultrapure water and diluted cDNA

sample. This reaction mixed was pipetted into a 96-well optical plate and vortexed on a Thermolyne Maxi-mix. The plate was spun down on a Beckman J2-HC centrifuge and inserted into an Applied Biosystems 7300 Real-Time PCR System. A SYBR Green absolute quantification program was run with the following cycles parameters: 1 cycle of 2 min. at 50 °C, 1 cycle 10 min. at 95 °C, 40 cycles of 15 sec. at 95 °C and 1 min. at 60 °C. A dissociation curve was run at the end of the program which consisted of the following: 15 sec. at 95 °C, 30 sec. at 60 °C, and 15 sec. at 95 °C. A standard curve was run using five-fold dilutions of total cDNA with each program. All candidate genes were run using SYBR-Green reagent. These genes were normalized to mouse Cyclophilin A (PPIA), which was assayed using a custom-made Taqman probe and primer mixture for PPIA, the Taqman Gene Expression PPIA Assay. There is no evidence to suggest that Cyclophilin A is directly or indirectly regulated by KLF genes. Here, 10 µL 2X Taqman PCR Master Mix was combined with 1 µL of the 20X Taqman Gene Expression Assay (PPIA). Here, RNA and ultrapure water were brought the reaction to 20 µL total volume. The samples were again loaded into a 96-well optical plate, vortexed, centrifuged, and placed in the 7300 Real-Time PCR System. Here, they were run on a FAM/TAMRA (acronoms for the reporter and quencher dyes, respectively) cycle which had the same temperature and time presets as the SYBR Green program without the dissociation curve due. When all data was gathered, the candidate gene mRNA quantities were divided by the PPIA mRNA quantities and the data was scaled by setting the WT average to a value of 1.

Chapter 3: Results

Breeding results suggest early death of KLF2/KLF4 DKO embryos.

Mouse embryos were dissected at E10.5 and E9.5 and genotyped as described previously (Table 4). At both ages, the progeny had the expected distribution of genotypes. As noted early, all E10.5 KLF2/KLF4 DKOs had no heartbeat and were dead by E10.5 (n=3), one with gross cranial bleeding. At E9.5 all KLF2-/-KLF4+/- (Figures 10G, 10H) and KLF2+/-KLF4-/- embryos (images not shown) had heartbeats and no gross cranial bleeding, while one of the DKOs had gross cranial hemorrhaging (n=12) (Figure 10I). While the number of embryos was not high enough to achieve statistical significance ($p \leq 0.05$) in a chi-square statistical test to determine time of embryonic death, the data suggest that KLF2/KLF4 DKO embryos die by E10.5, and that KLF2-/-KLF4+/- and KLF2+/-KLF4-/- embryos die around E10.5. Of note, death for these genotypes is sooner than either single knockout mouse. KLF4-/- mice die postnatally, while KLF2-/- mice die between E11.5 – E14.5, depending on specific knockout model and mouse genetic background.

E10.5

Genotype	Expected	Observed
WT	4	5
KLF2+/-	8	9
KLF4+/-	8	8
KLF2+/- KLF4+/-	16	14
KLF2-/-	4	3
KLF4-/-	4	3
KLF2-/- KLF4+/-	8	7 (3)
KLF2+/- KLF4-/-	8	12 (2)
KLF2-/- KLF4-/-	4	3* (1)

E9.5

Genotype	Expected	Observed
WT	8.4	13
KLF2+/-	16.8	16
KLF4+/-	16.8	16
KLF2+/- KLF4+/-	33.5	38
KLF2-/-	8.4	10
KLF4-/-	8.4	7
KLF2-/- KLF4+/-	16.8	9
KLF2+/- KLF4-/-	16.8	15
KLF2-/- KLF4-/-	8.4	10 (1)

Table 4: KLF2-/-KLF4-/- Knockout mice die by E10.5. All E10.5 DKO appeared dead (n=3) and one exhibited gross cranial bleeding. Three KLF2-/-KLF4+/- (n=7) and two KLf2+/-KLF4-/- (n=12) embryos had gross cranial bleeding. At E9.5, one DKO embryo exhibited gross cranial bleeding (n=12). Asterisks signify mice appeared dead without heartbeat. Parentheses include number with gross hemorrhage. E10.5 results are courtesy of Sean Fox, Megan Smith, and Aditi Chiplunkar. E9.5 breeding results were compiled by Gabriel Eades and Benjamin Curtis.

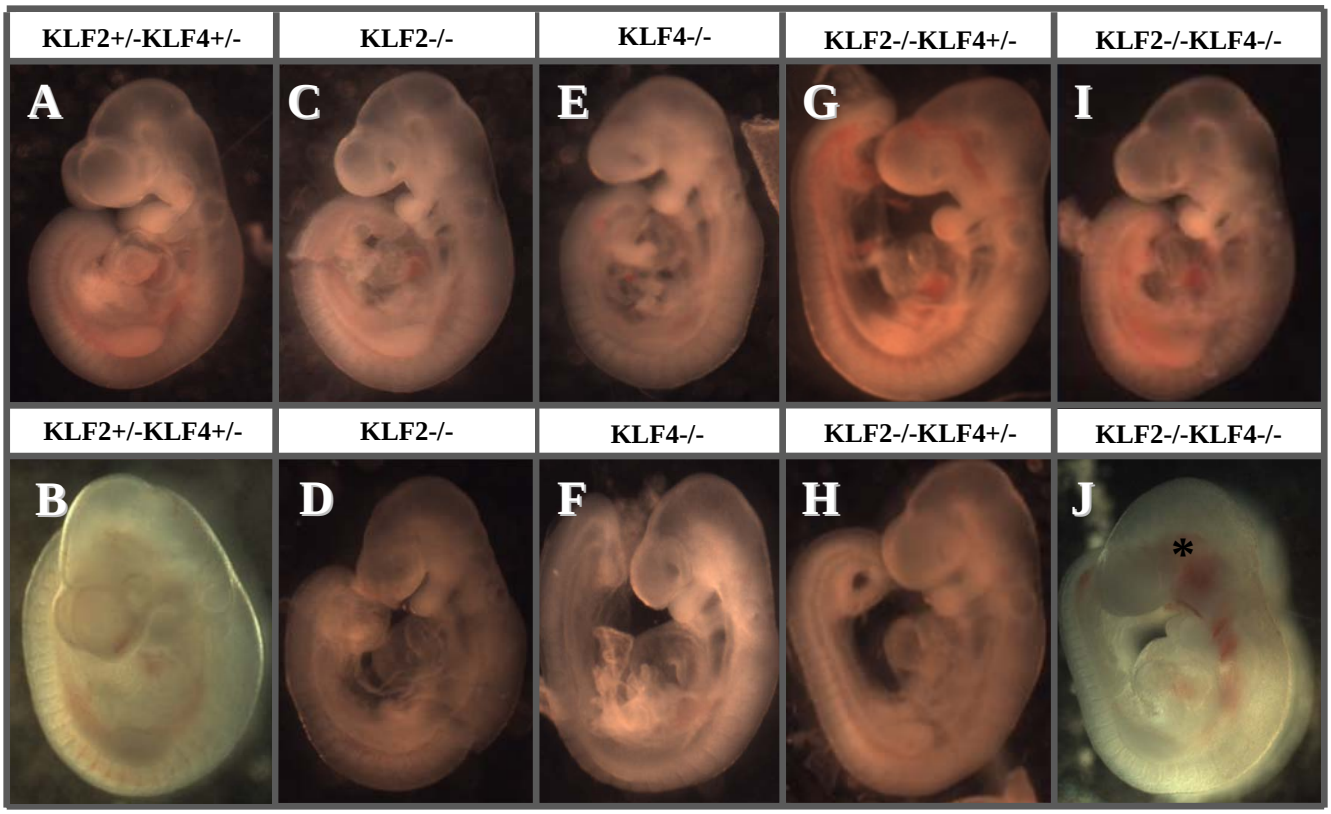

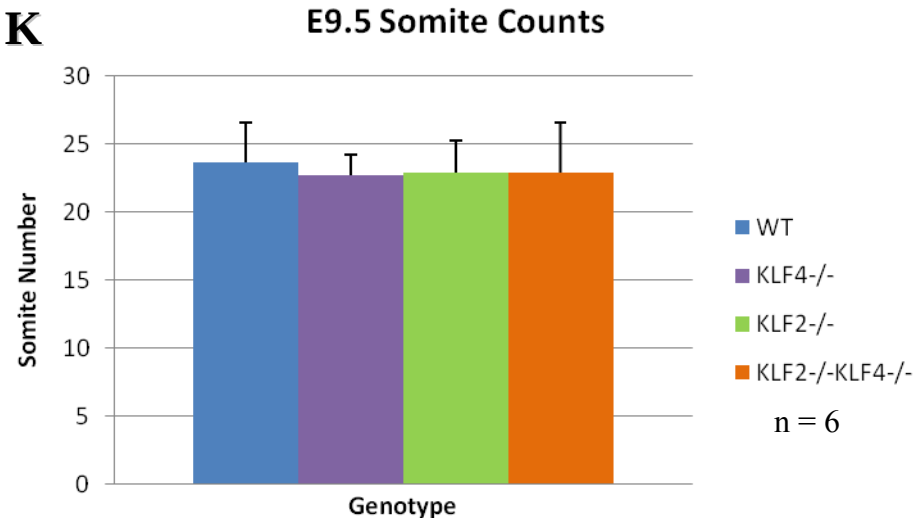

Figure 10: KLF2 KLF4 Knockout mice have a variable gross vascular phenotype at E9.5 but show no gross size difference or developmental delay. Asterisks identify cranial bleeds. One DKO was observed with gross cranial hemorrhaging (J) while the others appeared grossly normal (A-H). No difference was seen in somite counts across genotypes (K), where n = 6 for each genotype. Embryo numbers for internal reference include the following: A, #240; B, #167; C, #255; D, #272; E, #279; F, #280; G, #269; H, #262; I, #237; J, #168.

Whole-Mount Immunostaining with anti-PECAM antibody demonstrated that there were no gross capillary defects between E9.5 KLF2+/-KLF4+/-, KLF4-/-, KLF2-/-, and KLF2/KLF4 DKO embryos (Figure 11A-C). Anti-PECAM was used to stain the vasculature of the developing embryos. Unexpectedly, in embryos lacking KLF2, the posterior cardinal vein appeared to narrow as it moved caudally (arrows in Figure 11). This narrowing was observed in KLF2-/- embryos (Figure 11B), and even more dramatically in KLF2-/-KLF4-/- embryos (Figure 11C). Measurements taken of the posterior cardinal vein are indicated for KLF2+/-KLF4+/-, KLF4-/-, KLF2-/-, KLF2-/-KLF4+/-, and KLF2-/-KLF4-/-. No statistical test was undertaken due to the small sample size. As KLF2-/-KLF4+/- knockout mice had a high degree of variability, this may indicate that the phenotype is not always present or may be a reflection of low sample size. Another possible explanation for the narrowed posterior cardinal vein could include misrouting, where the vein moves towards the midline as it travels caudally, and is unable to be visualized by gross examination.

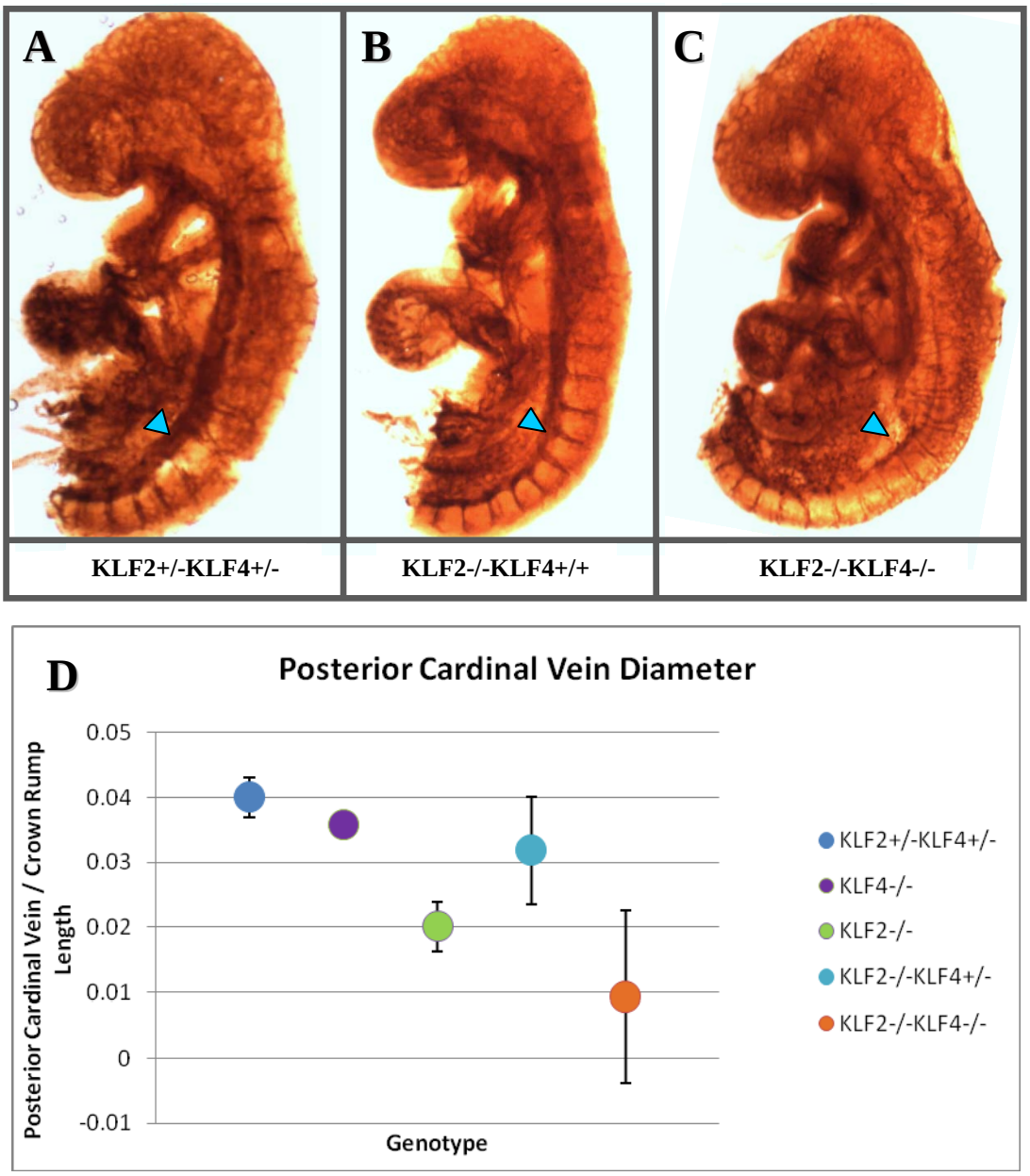

Figure 11: Posterior cardinal vein possibly narrower in E9.5 KLF2-/- mice. While no obvious capillary defects were noted with anti-PECAM immunostaining, the cardinal vein (arrows) appears to narrow while traveling from cranial to caudal when comparing KLF2+/-KLF4+/- (A) to KLF2-/- (B) and KLF2-/-KLF4-/- (C). The diameter of the posterior cardinal vein was quantified in various genotypes, standardized for crown rump length (D), where n = 2 for each genotype.

Hemorrhage and endothelial disruption in E9.5 KLF2/KLF4 DKO embryos

Transverse plastic sections of E9.5 embryos of the following genotypes were made: WT, KLF2+/-KLF4+/-, KLF2-/-, KLF4-/-, KLF2-/-KLF4+/-, KLF2+/-KLF4-/-, and KLF2-/-KLF4-/-. A phenotype was observed in both KLF2-/-KLF4-/- and KLF2-/-KLF4+/- embryos, but it was variable. The KLF2/KLF4 DKO that had shown gross hemorrhage in whole-mount (embryo #168), had bleeding in the head, beginning rostrally at the level of optic vesicle and ending caudally at the level of the first branchial arches (Figure 12G-K). At all levels, hemorrhaging in this embryo was confined to the primary head vein (PHV) and the rostral portion of the anterior cardinal vein, into which the PHV drains. Bleeding penetrated at some levels, all the way to the midline, infiltrating the supporting cranial mesenchyme, a precursor tissue to vascular smooth muscle. Figure 12A-F shows images of KLF2+/-KLF4+/- (embryo #167) and KLF2-/- (embryo #7) sections that indicate intact vasculature at the same level as embryo #167. While only one E9.5 KLF2/KLF4 DKO embryo at this age (n=12) showed gross bleeding, nine E9.5 KLF2/KLF4 DKO embryos (9 out of 12) showed endothelial disruption of the PHV at the level of the optic vesicle in transverse section (Figure 13), making this a common finding. In these embryos, erythrocytes were visualized outside the lumen of the PHV, with apparent gaps between joining endothelial cells. No obvious reduction in surrounding mesenchyme was seen. Endothelial disruption of the PHV was also seen in two KLF2-/-KLF4+/- embryos (n=4) (Figure 14) as observed at E10.5. While gaps were more difficult to identify in the KLF2-/-KLF4+/- sections, the presence of erythroid cells localized outside of the PHV lumen, confirmed that the endothelial layer was lacking continuity (Figure 14B, 15D, 15F). No abnormal phenotype was seen in KLF2+/-KLF4-/- embryos, indicating that KLF2 ablation may be required for the abnormal vascular phenotype.

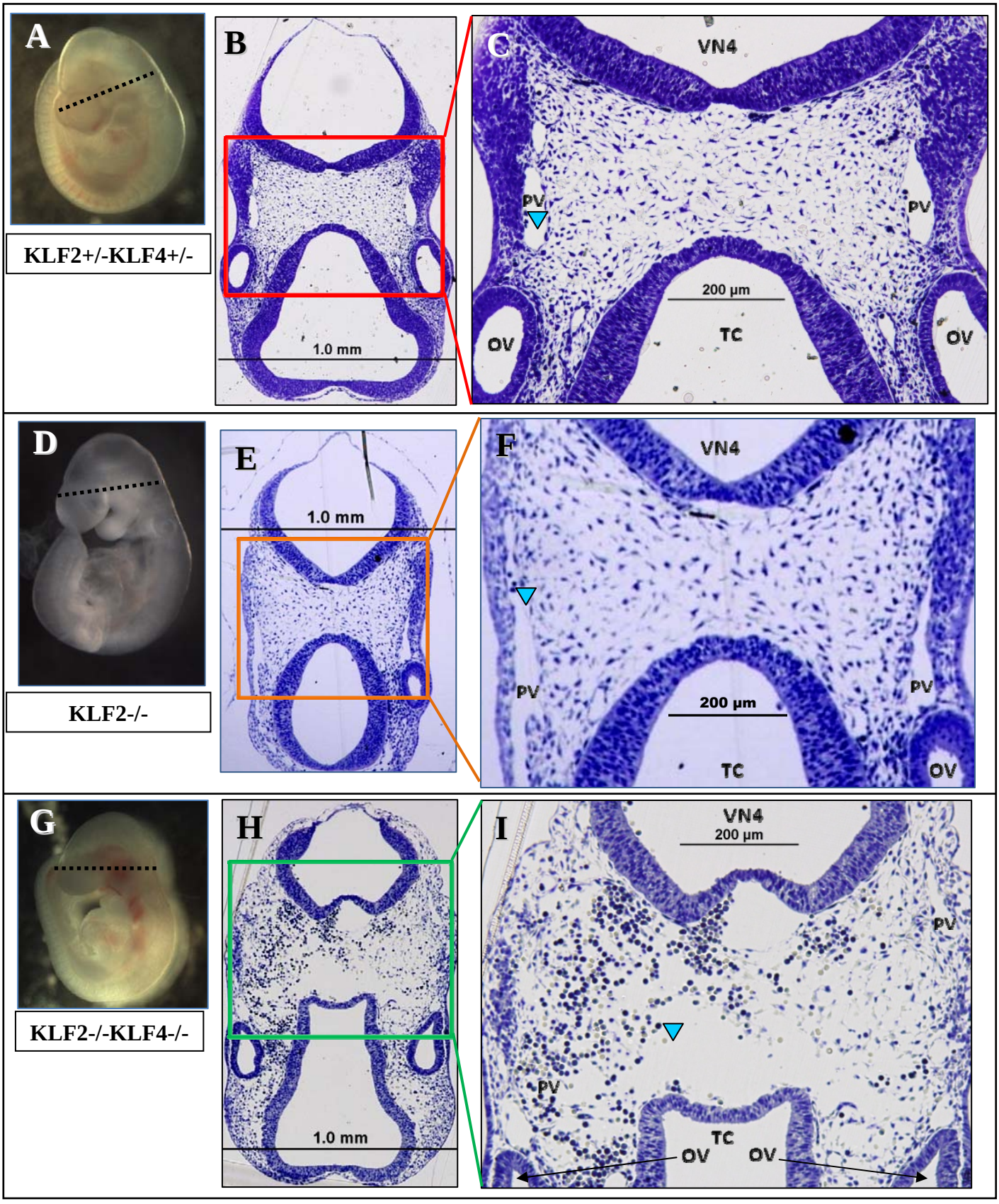
A
B
C
VN4
PV
PV
PV
200 µm
TC
OV
OV
1.0 mm
KLF2+/-KLF4+/-
D
E
F
VN4
1.0 mm
PV
PV
200 µm
TC
OV
KLF2-/-
G
H
I
VN4
200 µm
PV
PV
TC
OV
OV
1.0 mm
KLF2-/-KLF4-/-

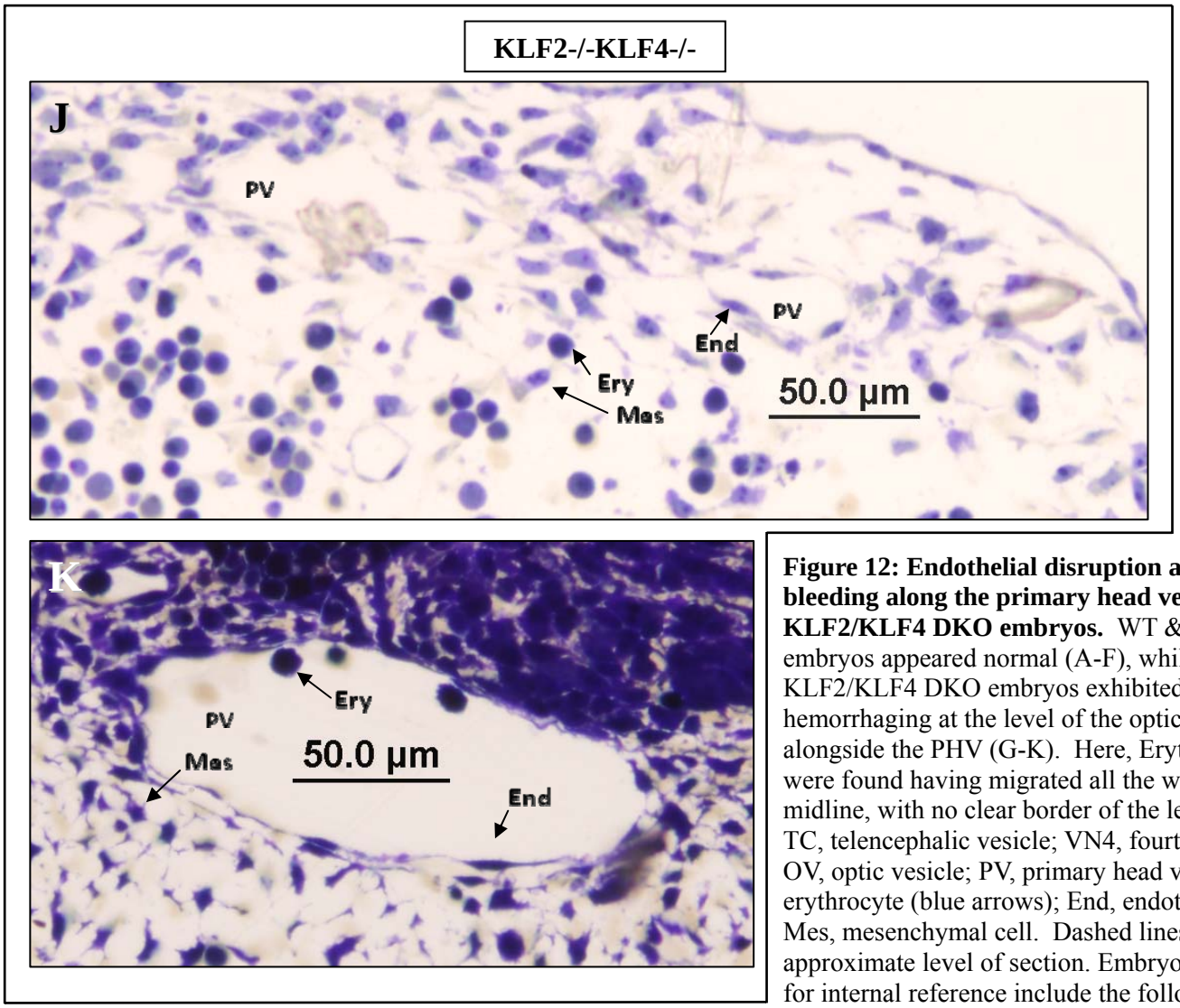

Figure 12: Endothelial disruption and bleeding along the primary head vein in E9.5 KLF2/KLF4 DKO embryos. WT & KLF2-/- embryos appeared normal (A-F), while KLF2/KLF4 DKO embryos exhibited clear hemorrhaging at the level of the optic vesicle alongside the PHV (G-K). Here, Erythrocytes were found having migrated all the way to the midline, with no clear border of the left PHV. TC, telencephalic vesicle; VN4, fourth ventricle; OV, optic vesicle; PV, primary head vein; Ery, erythrocyte (blue arrows); End, endothelial cell; Mes, mesenchymal cell. Dashed lines indicate approximate level of section. Embryo numbers for internal reference include the following: A-C, #167; D-F, #7, G-I, #168.

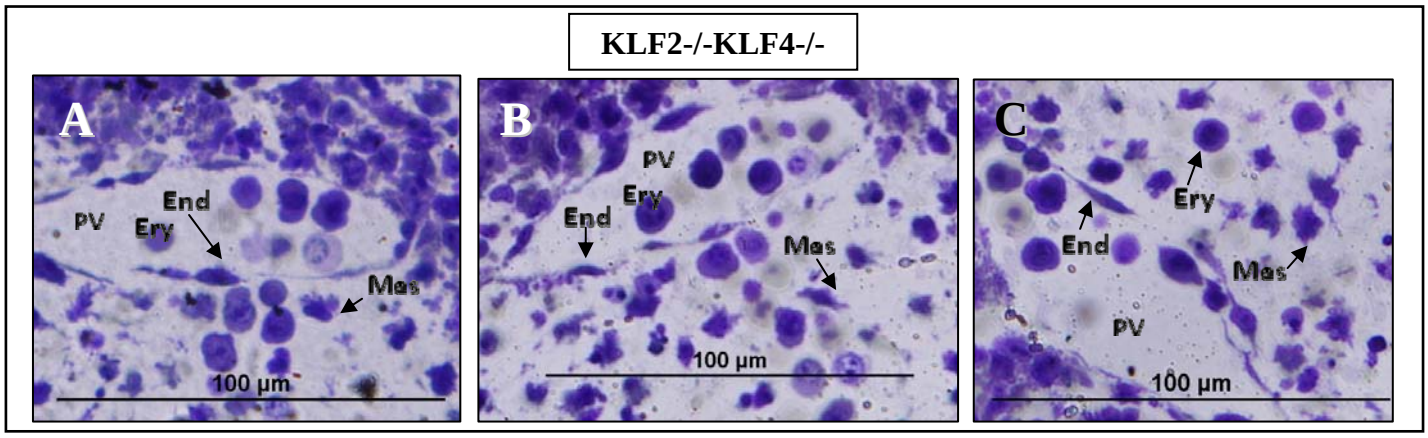

Figure 13: Additional sections showing less severe phenotype in some E9.5 KLF2/KLF4 DKOs. WT & KLF2-/- embryos appeared normal, while KLF2/KLF4 DKO embryos exhibited discontinuity of the endothelial layer border at the level of the optic vesicle alongside the PHV. Here, erythrocytes were found outside the vessel lumen. TC, telencephalic vesicle; VN4, fourth ventricle; OV, optic vesicle; PV, primary head vein; Ery, erythrocyte; End, endothelial cell; Mes, mesenchymal cell. Embryo numbers for internal reference include the following: A-C, #206.

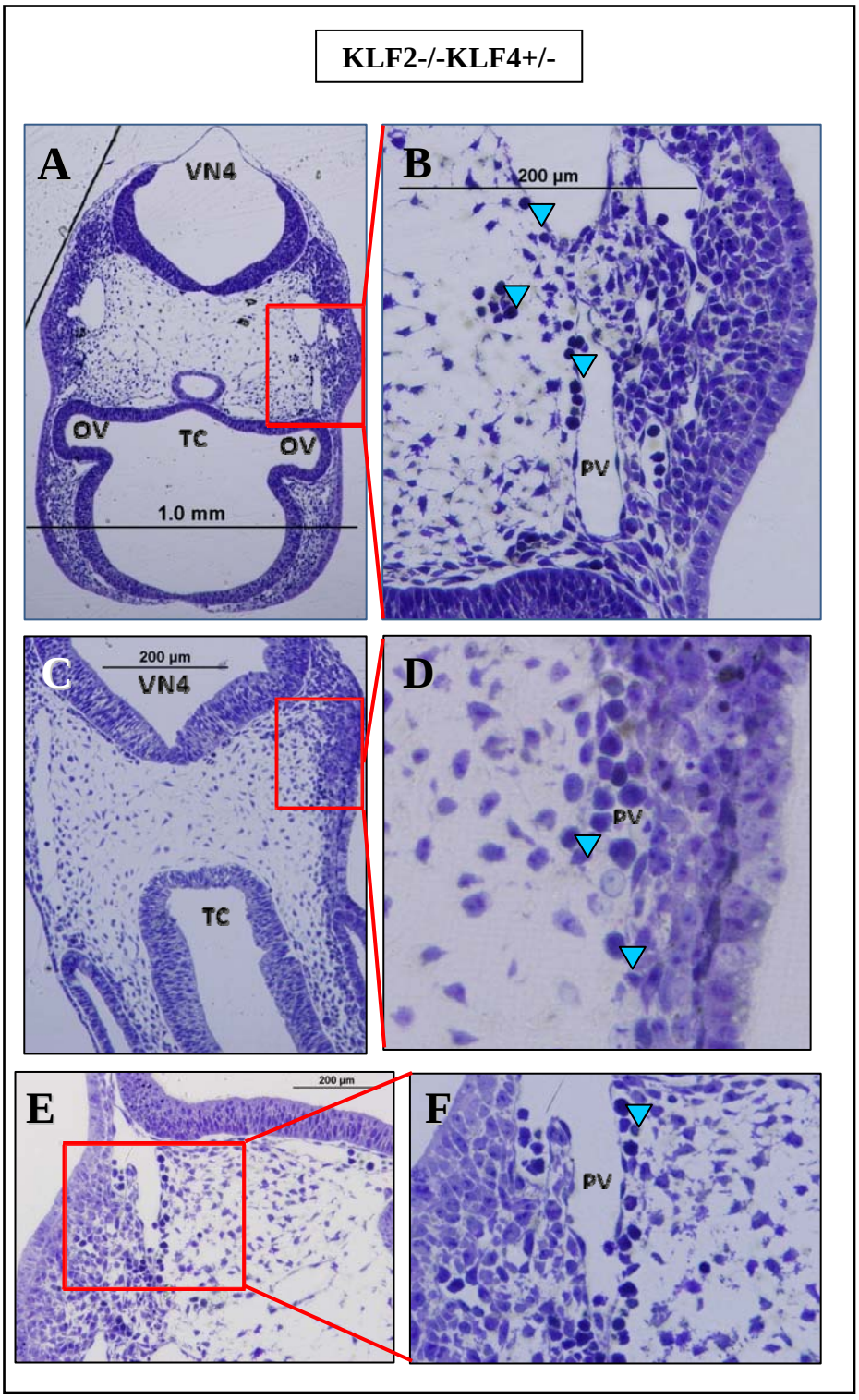

Figure 14: Additional sections showing less severe phenotype in some E9.5 KLF2-/-KLF4+/- embryos. KLF2-/-KLF4+/- embryos showed similar endothelial disruption to KLF2/KLF4 DKOs (Figure 13) with erythrocytes localized outside of the PHV at the level of the optic vesicle. TC, telencephalic vesicle; VN4, fourth ventricle; OV, optic vesicle; PV, primary head vein; Ery, erythrocyte (blue arrows); End, endothelial cell; Mes, mesenchymal cell. Embryo numbers for internal reference include the following: A-B, #194; C-D, #126; E-F, #195.

Electron micrographs further define the phenotype in the primary head vein in KLF2/KLF4 DKO embryos at E9.5.

Electron micrographs of the PHV at the level of the optic vesicle are shown in Figure 15. In the WT (embryo #330, n=1), the endothelium was generally continuous with gaps ≤ 5 μm (Figure 15A). The typical flattened spindle shape of the endothelial cells seen at the light level was preserved. The KLF4-/- embryo (embryo #307, n=1) was also generally continuous with gaps ≤ 2 μm, and was otherwise, indistinguishable from the WT (Figure 15C). KLF2-/- embryos (n=2) had a variable phenotype. KLF2-/- (1, embryo #126) had no visible abnormalities of the endothelium, appearing identical to the WT and KLF4-/- embryos, with gaps ≤ 3 μm (Figure 15B). Conversely, KLF2-/- (2, embryo #3) had extended, frequent gaps ≤ 7.5 μm along only the medial and not lateral aspect of the vessel (Figure 15D). The endothelial cell bodies appeared present, and are obviously outlining the lumen of the PHV. KLF2/KLF4 DKO embryos (embryos #328 and #331, n=2) had endothelial disruption and more frequent gaps up to 20 μm on both the medial and lateral aspects of the fragmented vessel wall (Figure 15E, F, I). Filopodia-like cytoplasmic projections extend from the endothelial cell bodies (Figure 15G, H), which were not observed in either KLF2-/- embryo. In KLF2/KLF4 DKO embryos, there are also numerous vacuoles in the cell cytoplasm not observed in any other genotype. Lastly, the endothelial cells in the KLF2/KLF4 DKOs took on a more bulbous shape compared to KLF2-/-, KLF4-/- and WT. The KLF2-/- and KLF2-/-KLF4-/- endothelial cells are wider than KLF4-/- and WT, although the sample size was too small to perform a statistical test (Figure 16). As it was postulated that KLF2-/- and KLF2-/-KLF4-/- may have reduced cytoplasm but the same cell number, the cytoplasmic coverage of the PHV endothelium luminal boarder was calculated compared to the longitudinal distance spanned by the cell nuclei. A steep gradient from WT to KLF2-/-, to KLF2-/-KLF4-/- was observed (Figure 17). However, no statistical test was

undertaken due to (1) the small sample size and (2) possible variation in the section orientation, both of which might inflate the ratio seen in the mostly longitudinal sections of WT and KLF4-/-. These findings confirm the disruption of the endothelial layer seen at the light microscopy level for E9.5 KLF2/KLF4 DKO embryos, and refine the description of the phenotype.

The images in Figure 17 include endothelial cells pseudo-colored with image editing software. Endothelial cells were selected and colored based on the appearance of a continuous or semi-continuous endothelial layer immediately adjacent to the PHV lumen, and when applicable, the presence of gap junctions between neighboring endothelial cells.

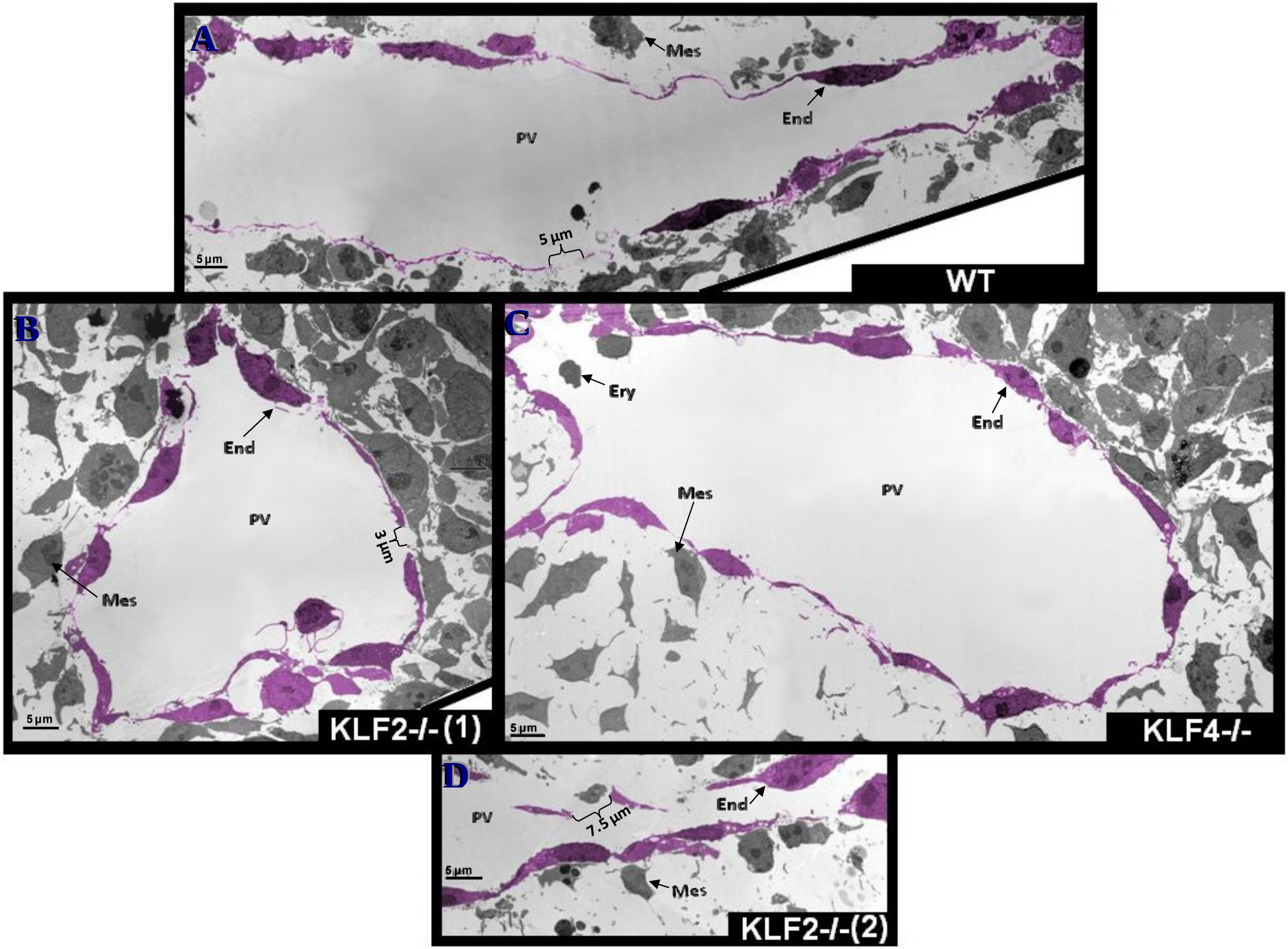
A
Mes
End
PV
5 µm
5 µm
WT
B
End
PV
3 µm
Mes
5 µm
KLF2-/-(1)
C
Ery
End
Mes
PV
5 µm
KLF4-/-
D
PV
7.5 µm
End
5 µm
Mes
KLF2-/-(2)

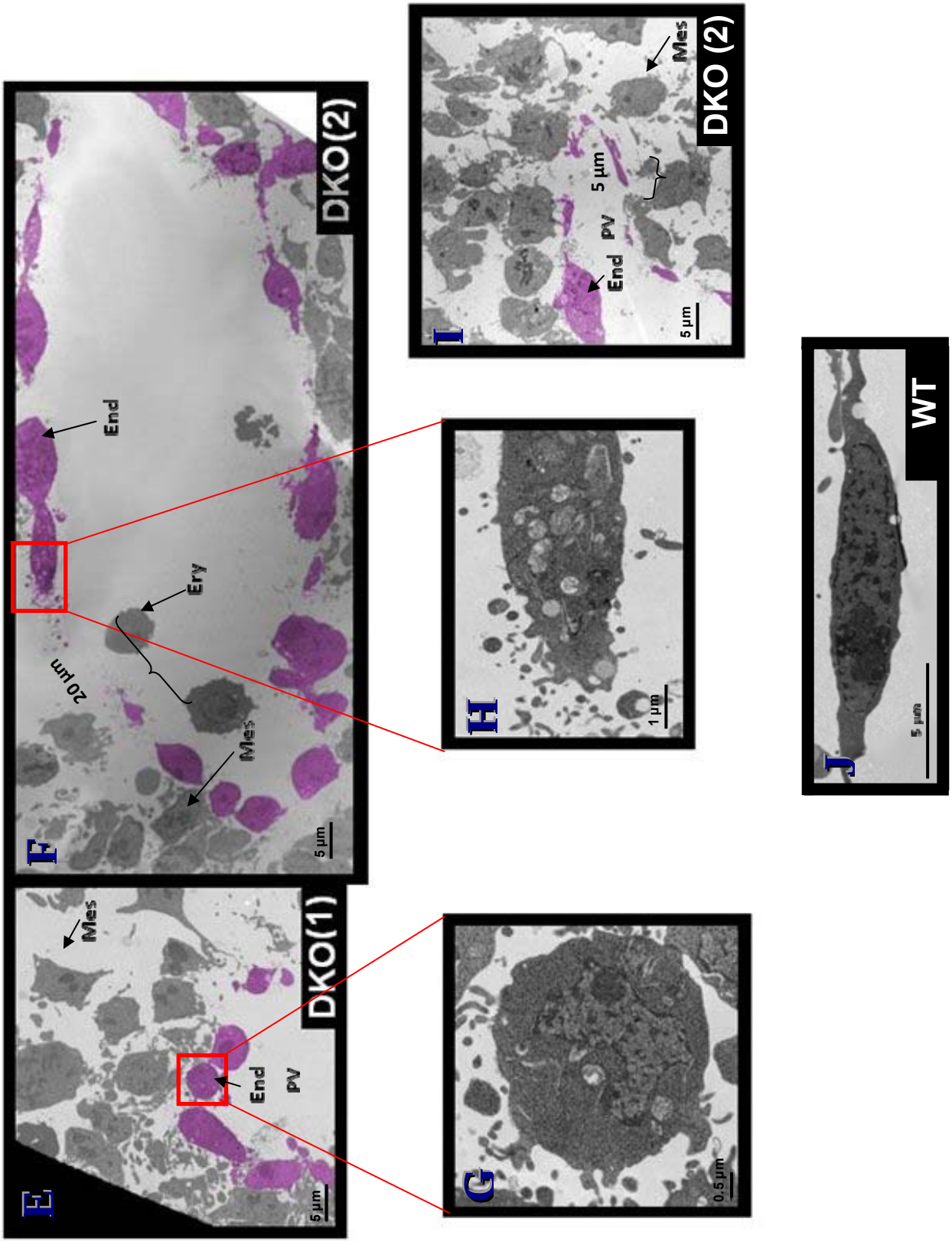
F
DKO(2)
End
Ery
Mes
20 µm
5 µm
E
DKO(1)
Mes
End
PV
5 µm
H
1 µm
G
0.5 µm
I
DKO (2)
Mes
5 µm
PV
End
5 µm
J
WT
5 µm

Figure 15: Electron micrograph of transverse sections of E9.5 embryos. Images were taken of the primary head vein at the level of the optic vesicle. The endothelial cell layer was pseudo-colored using GIMP (GNU Image Manipulation Program) version 2.6 open-source digital photo editing software. (A-F, J) 1,200X, (G) 5,000X, (H) 8,000X. (A, J) The WT embryo (n=1) maintained a continuous endothelial layer with slight gaps less than 1 micron in length. (C) No gaps were observed in KLF4-/- embryos (n=1). (B, D) KLF2-/- embryos (n=2) presented a variable phenotype between given embryos. (E-I) KLF2/KLF4 DKO embryos (n=2) had a consistent breakdown of the endothelial membrane. PV, primary head vein lumen; Ery, erythrocyte; End, endothelial cell; Mes, mesenchymal cell. Embryo numbers for internal reference include the following: A, #330; B, #126; C, #307; D, #3; E, #328; F, #331; G, #328; H-I, #331; J, #330.

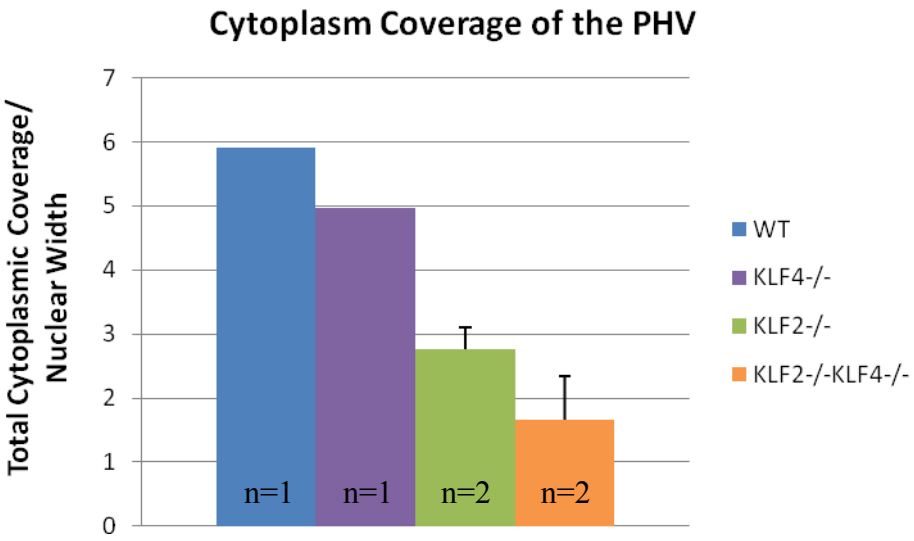

Figure 16: E9.5 KLF2-/-, KLF2-/-KLF4-/- mice may have increased diameter of endothelial cells in the primary head vein. Following the PHV endothelial luminal border, the endothelial cell width was measured from apical membrane through the nucleus, to the basolateral membrane. Only cells with defined nuclei were assayed. These results are consistent with the bulbous-looking endothelial layers observed in KLF2-/- and KLF2-/-KLF4-/- mice. The number of cells measured per genotype includes Wt, 9; KLF4-/-,14; KLF2-/-, 15, DKO, 23. Due to the small sample size and possible variability in plane of section in the images, no statistical test was attempted.

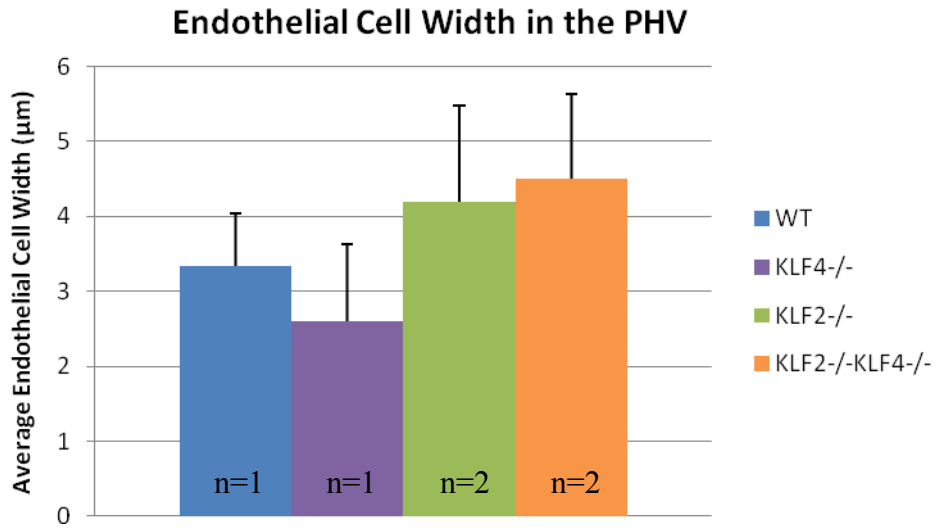

Figure 17: E9.5 KLF4-/-, KLF2-/-, and KLF2-/-KLF4-/- mice may have reduced endothelial cell cytoplasm in the primary head vein. Following the PHV endothelial luminal border, endothelial cytoplasm length compared to nuclear diameter was tabulated for WT, KLF4-/-, KLF2-/-, and KLF2-/-KLF4-/-, showing a possible reduction in the endothelial cell cytoplasm, consistent with the gaps seen in EM micrographs. KLF2-/- and KLF2-/-KLF4-/- mice. The number of cells measured per genotype includes Wt, 9; KLF4-/-, 14; KLF2-/-, 15, DKO, 23. Due to the small sample size and possible variability in plane of section in the images, no statistical test was attempted.

Cell counts reveal reduced midline mesenchymal density in KLF2/KLF4 DKOs at E9.5.

Using the light microscopy digital photographs taken of serial sections of E9.5 embryos, mesenchymal density was determined for the midline and directly medial to the PHV at the level of the optic vesicle. A pre-determined area was selected at the midline or adjacent medially to the PHV where cells were counted. No significant differences were observed in mesenchymal density immediately medial to the PHV for KLF2/KLF4 DKOs, KLF2-/-KLF4+/-, or KLF2-/- compared to KLF2+/-KLF4+/- (Figure 18A). When counts were taken in a prescribed area at the midline, KLF2/KLF4 DKOs had significantly fewer cells than KLF2+/-KLF4+/- and KLF2-/- in paired student t-tests, with p-values of 0.049 and 0.011 respectively (Figure 18B). Mesenchymal density counts along the PHV at E10.5 at the level of the optic vesicle revealed no significant differences between genotypes (Figure 18C).

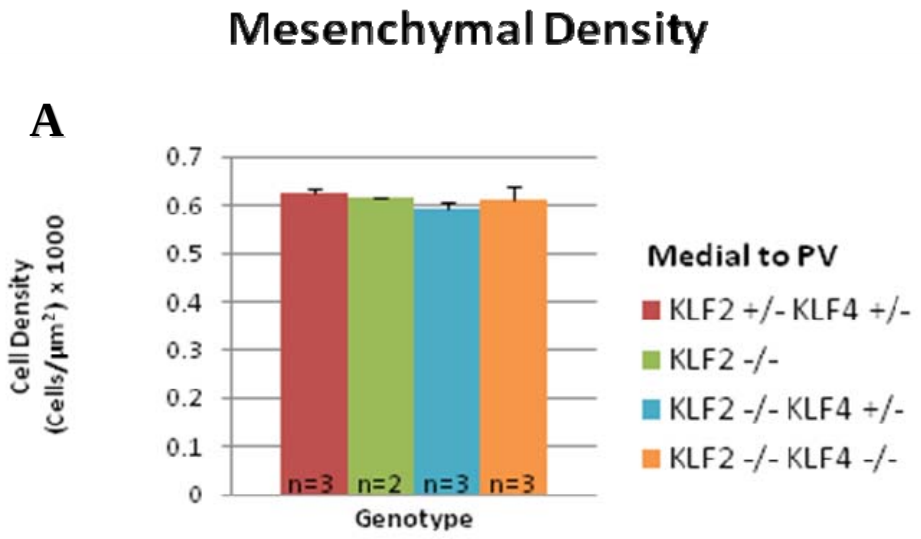
Mesenchymal Density
A
Cell Density (Cells/μm²) x 1000
0.7
0.6
0.5
0.4
0.3
0.2
0.1
0
n=3
n=2
n=3
n=3
Genotype
Medial to PV
KLF2 +/- KLF4 +/-
KLF2 -/-
KLF2 -/- KLF4 +/-
KLF2 -/- KLF4 -/-

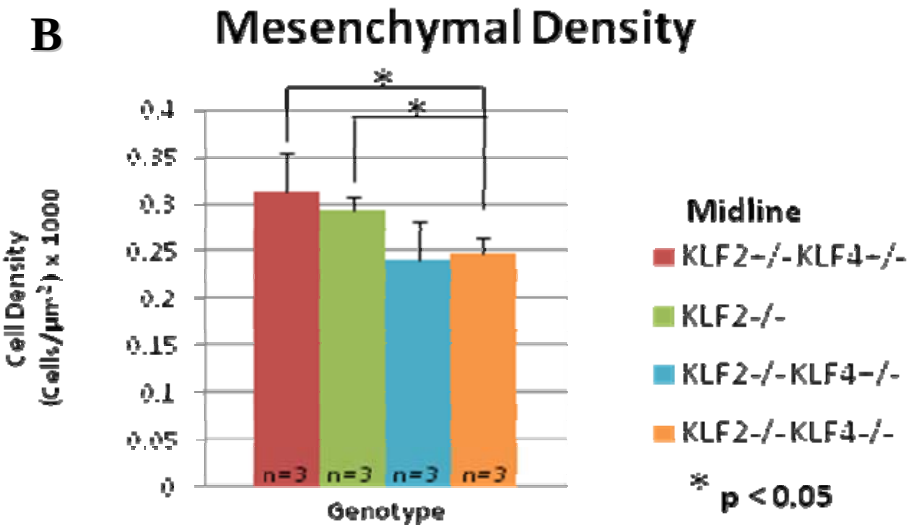
B
Mesenchymal Density
*
*
Cell Density (Cells/μm²) x 1000
0.4
0.35
0.3
0.25
0.2
0.15
0.1
0.05
0
n=3
n=3
n=3
n=3
Genotype
Midline
KLF2-/-KLF4-/-
KLF2-/-
KLF2-/-KLF4-/-
KLF2-/-KLF4-/-
* p < 0.05

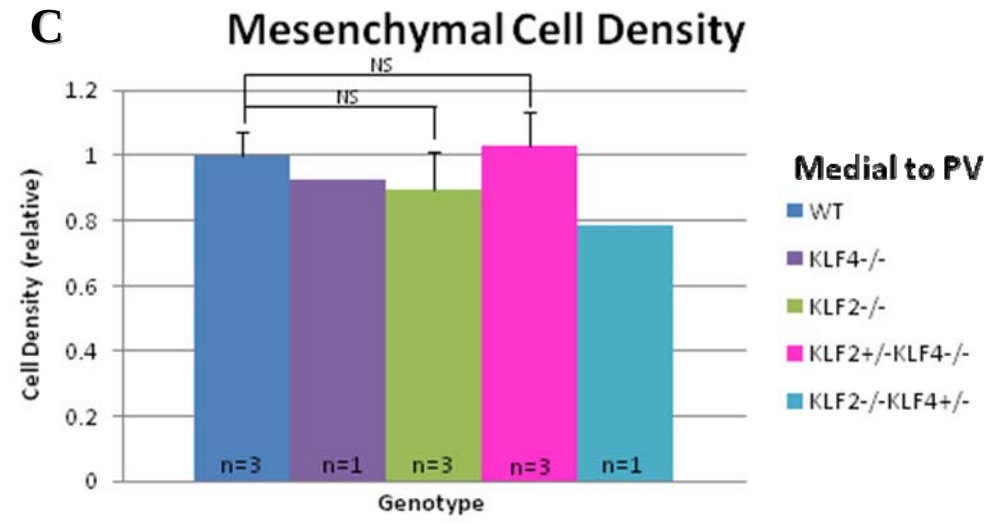
C
Mesenchymal Cell Density
NS
NS
Cell Density (relative)
1.2
1
0.8
0.6
0.4
0.2
0
n=3
n=1
n=3
n=3
n=1
Genotype
Medial to PV
WT
KLF4-/-
KLF2-/-
KLF2+/-KLF4-/-
KLF2-/-KLF4+/-

Figure 18: Cranial mesenchyme density of E9.5 and E10.5 embryos. No difference between genotypes was observed when mesenchymal density was tabulated medial to the PHV at the level of the optic vesicle in transverse section at E9.5 (A). When counts were taken at the midline at E9.5 (B), KLF2/KLF4 DKOs had significantly fewer cells than KLF2+/-KLF4+/- ($p = 0.049$) and KLF2-/- ($p = 0.011$) in paired student t-tests. No difference between genotypes was observed when mesenchymal density was tabulated medial to the PHV at the level of the optic vesicle in transverse sections at E10.5 (C).

KLF2 RNA is expressed in endothelial cells of the primary head vein in E10.5 embryos.

In order to elucidate the molecular mechanism contributing to the phenotype observed in KLF2/KLF4 DKO embryos, localization of KLF2 and KLF4 transcript at the level of the optic vesicle in E10.5 embryo was attempted. In-situ hybridization localized KLF2 mRNA to both endothelial cells and erythrocytes in the PHV of E10.5 FVB/N WT embryos. Antisense KLF2 RNA probe (T3-K2-439) binding was visualized with anti-digoxigenin AP product (Figure 19A, B) and compared to serial tissues exposed to KLF2 RNA sense probe (T7-K2-439) control (Figure 19C, D). The blue arrows in Figure 19B point out the hybridization taking place in endothelial cells, both medially and laterally. Yellow arrows indicate apparent hybridization of expressed KLF2 mRNA in erythrocytes, as previously shown by qRT-PCR assays (Basu, 2004). Darkened erythrocytes in Figure 19D appeared more intense due to the heightened contrast, and represent a negative result as is typically seen with nuclear fast red when viewed with the compound light microscope. Additional serial sections exposed to sense controls displayed background staining of similar and greater intensity to the section treated with antisense probe. However, these sections were slightly less intact than those pictured, and hence not as informative. The additional KLF2 and KLF4 probes described in the method section failed to present consistent, clear results and will be replicated in future studies.

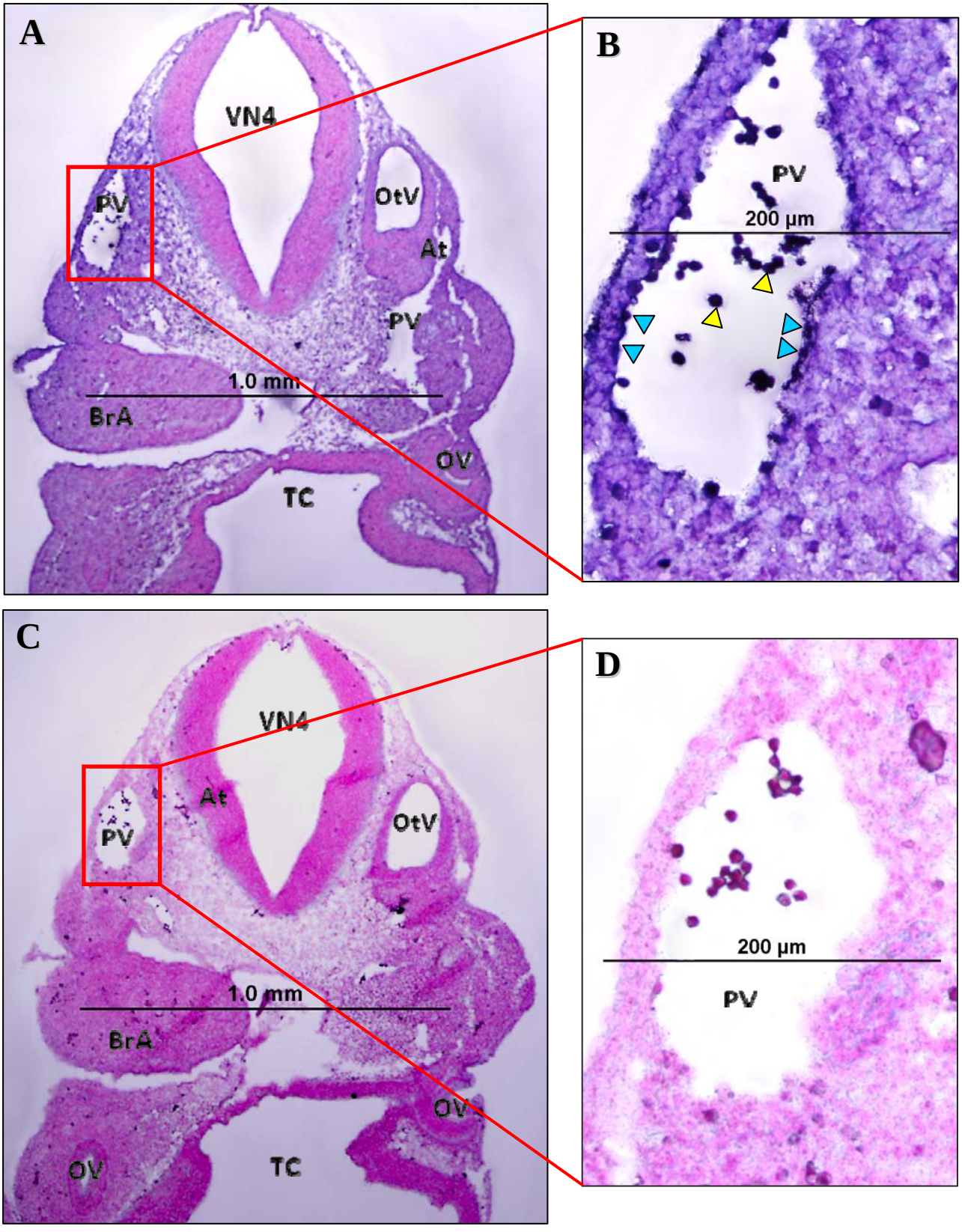
A
VN4
PV
OtV
At
PV
1.0 mm
BrA
OV
TC
B
PV
200 µm
C
VN4
At
PV
OtV
1.0 mm
BrA
OV
OV
TC
D
200 µm
PV

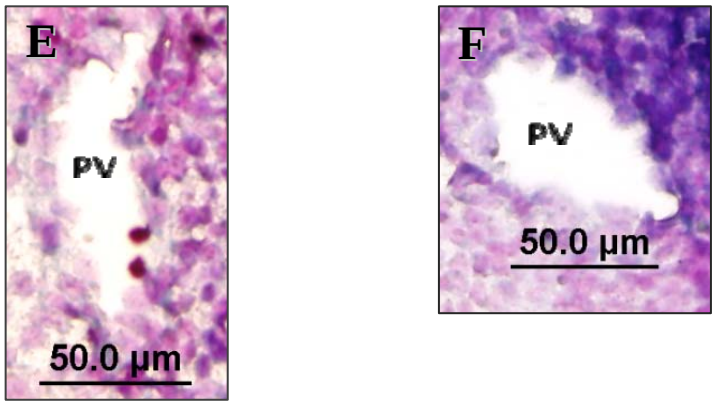

Figure 19: Localization of KLF2 mRNA to the endothelium of the primary head vein at E10.5. KLF2 RNA antisense probe hybridized to endothelial cells (blue arrows) and blood cells (yellow arrows) of the PHV (A, B). KLF2 RNA sense probe control showed no hybridization to any cell types (C, D, E, F). TC, telencephalic vesicle; VN4, fourth ventricle; OV, optic vesicle; PV, primary head vein; OtV, otic vesicle; BrA, first branchial arch; Ery, erythrocyte; End, endothelial cell; Mes, mesenchymal cell; At, tissue artifact (fold/tear).

KLF2 and KLF4 regulate eNOS mRNA expression in E9.5 whole embryo.

Expression of eNOS mRNA in E9.5 mouse whole embryo was quantified and standardized to the ubiquitously-expressed housekeeping gene, cyclophilin A (Figure 20). While no difference in eNOS mRNA expression was noted between WT and KLF2-/-, the KLF2+/-KLF4+/- and KLF4-/- embryos appear to show a reduction compared to WT. In a two-tailed student t-test, eNOS mRNA expression in KLF2/KLF4 DKOs was significantly lower than in KLF2-/- ($p = 0.0046$) and KLF4-/- (0.0026) embryos. The gradient of eNOS mRNA expression between genotypes suggests that KLF4 plays a greater role than does KLF2 in eNOS regulation. This view is further supported by the observance that KLF2-/- embryos had greater eNOS expression than KLF2+/-KLF4+/- mice. As WT expression of eNOS mRNA was highly variable, possibility due to small sample size, it was not significantly different than KLF4 expression of eNOS mRNA.

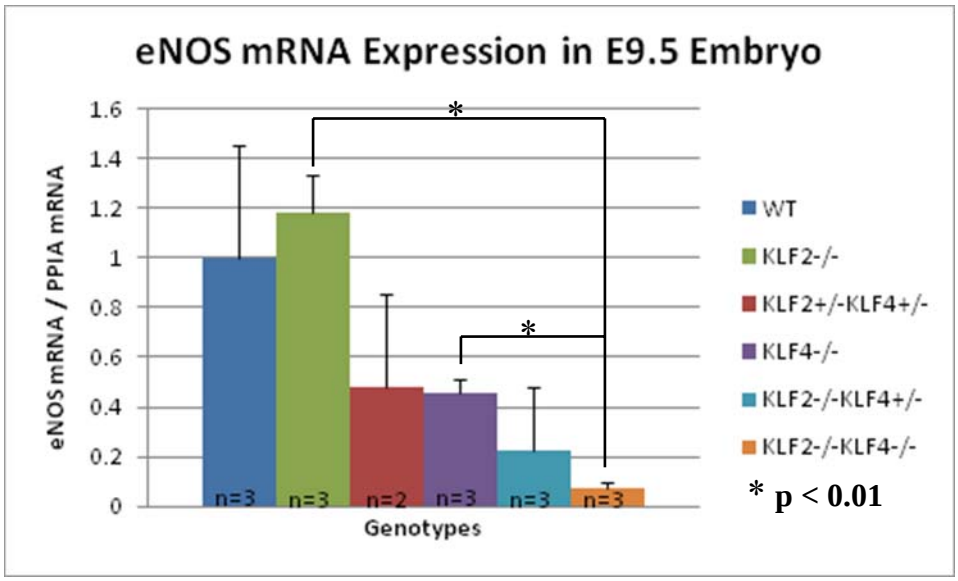

Figure 20: KLF2 and KLF4 gene ablation decreases eNOS mRNA expression. qRT-PCR revealed that eNOS mRNA was down-regulated in E9.5 KLF2-/-KLF4-/- embryos compared to KLF2-/- and KLF4-/- embryos of the same age. Additionally, KLF4-/- expression of eNOS was significantly less than KLF2-/- eNOS expression.

Chapter 4: Discussion

Earlier death of KLF2/KLF4 DKO embryos indicates more severe phenotype than KLF2-/- or KLF4-/- embryos

KLF2-/-KLF4-/- embryos die by E10.5, which is earlier than the reported death of KLF2 KOs at E11.5-E14.5 (Kuo, 1997; Wani, 1998; Lee, 2006; Chiplunkar, unpublished data). KLF4 KO mice die post-natally. The KLF2/KLF4 DKO phenotype included gross and microscopic hemorrhaging, which was also observed in E10.5 KLF2-/-KLF4-/+, E9.5 KLF2-/-KLF4-/-, and E9.5 KLF2-/-KLF4+/- mutants. The graded increase in severity of cranial hemorrhage between E10.5 KFL2-/-KLF4+/- and E10.5 KLF2-/-KLF4-/- shows how the loss of one additional KLF gene impacts the vascular development of the mouse embryo. This effect of gene dosing is seen in mice with mutated Hox genes, namely Hoxa-13 and Hoxd-13 (Warot, 1997). Here, the combined effect of knocking out both genes is embryonic lethality. The mice of genotype Hoxa-13+/-Hoxd-13-/- reach adulthood but with more severe abnormalities of the genitourinary and digestive systems than seen in Hoxa-13-/- mutants or Hoxa-13+/-Hoxd-13+/- double heterozygotes. Interestingly, Hoxa-13-/-Hoxd-13+/- mutants die *in utero* like Hoxa-13-/-Hoxd-13-/- mice, indicating that Hoxa-13 may play a greater role in the phenotype than Hoxd-13. Ablation of KLF2 disproportionately affects vascular development in the mouse embryo compared to KLF4, as discussed further below.

WT, KLF2-/-, and KLF2-/-KLF4-/- illustrate a gradient of phenotypes

As expected, E9.5 KLF4-/- embryo morphology closely resembles WT in the PHV, with few gaps and a normal representation of spindle-shaped, flattened endothelial cells. Unexpectedly, when examined using electron microscopy, E9.5 KLF2-/- embryos presented a variable phenotype. This phenotype, while present in one of two KLF2-/- embryos, was one-

sided, medially. E9.5 KLF2-/-KLF4-/- embryos showed bilateral gaps larger than those in KLF2-/- mutants, large enough for an E9.5 primitive erythrocyte, averaging 16 – 17 μm to escape the lumen of the primary head vein (Fraser, 2007). Additionally, the endothelium of the KLF2-/-KLF4-/- embryos had numerous cytoplasmic projections, similar in appearance to the filopodia present in migratory cells. Interestingly, VEGF has been shown to guide angiogenic sprouting through the use of filopodial extension of endothelial tip cells (Gerhardt, 2003), or the cells that form the tip of sprouting blood vessels. This response also involves VEGFR2, VEGFR3, and NRP—all established VEGF receptors (Reviewed by De Smet, 2009). Furthermore, endothelial tip cell competition, or competition between endothelial cells for positioning as a tip cell is regulated by the glycosylation of Notch receptors and their ligands, Jagged1 and Delta-like 4 (Benedito, 2009). Interestingly, Jagged1-/- mice die *in utero* at E11.5 due to vessel hemorrhaging, suggesting that it may be an ideal candidate for KLF2 and KLF4 regulation (Xue, 1999).

The preferential sidedness of hemorrhaging along the PHV may be caused by either physics, molecular biology, or both. Lateral to the PHV lies the trigeminal neural crest tissue that extends slightly into the first branchial arches at E9.5. By E10.5 the tissue has further developed into the trigeminal ganglion and has migrated out of the branchial arches (Kaufmann, 1992). At both stages, this dense pre-neuronal tissue is highly cellular, forming a dense framework of cells, typical of neuronal tissue in the adult. The high cell density may provide physical support in contrast to the cranial mesenchyme, located medially to the vessel. On the other hand, KLF4 RNA has been localized *in vivo* to both cranial epithelium and the underlying mesenchyme at E10.5 (Ehlermann, 2003), suggesting that it may act as a transcriptional regulator in the mesenchyme, which brackets the medial vessel border. In this scenario, KLF4 would

regulate genes in the mesenchyme that affect vessel support, in coordination with the downstream effectors of KLF2.

One unforeseen observation was the small gaps in both WT and KLF4 mutants along the PHV using electron microscopy. These breaks may be characteristic of vessel fenestration, traditionally observed in the endocrine, renal**,** intestinal**,** and liver capillaries of adult mice. Interestingly, VEGF has been shown via electron microscopy to induce fenestration in both capillaries and post-capillary venules when administered to adult rats (Roberts, 1995). While venous fenestration during development has not been documented, the prominent angiogenic role of VEGF suggests that vessel fenestration may be occurring during embryogenesis, particularly given the rapidly-changing nutritional needs and tissue morphogenesis that is required to support the growing fetus. On the other hand, the combination of fixation, dehydration, clearing, and embedding may be too severe a mechanical and biochemical set of treatments for the thin endothelial cell layer to remain fully continuous in all areas of the primary head vein. It should be re-emphasized, however, that despite this possible limitation, KLF2-/- and KLF2-/-KLF4-/- had larger gaps along the primary head vein than WT or KLF4-/- embryos, and cytoplasmic projections were only seen in KLF2-/-KLF4-/- embryos.

Phenotype in E9.5 KLF2/KLF4 DKO has similarities with E9.5 EKLF/KLF2 DKO.

The phenotype observed in KLF2/KLF4 DKOs had interesting similarities to that of EKLF/KLF2 DKO embryos. More specifically, E9.5 EKLF/KLF2 DKO endothelial cells in the dorsal aorta sometimes appeared partially detached from the underlining mesenchyme and bulbous compared to WT, EKLF-/-, and KLF2-/- (Lung, 2008). In the E9.5 EKLF/KLF2 DKO yolk sac, endothelial cells sent out cytoplasmic, filopodia-like projections into the lumen of blood islands, in contrast to the smooth, non-projecting endothelium of WT yolk sac (Basu,

2007). These data, in addition to the more severe phenotype observed in E9.5 KLF2-/-KLF4+/- mice than in KLF2+/-KLF4-/-, may again indicate that KLF2 plays the major regulatory role(s) since the lack of KLF2 gives rise to the abnormal endothelial morphology.

Hemorrhage and death despite normal gross vasculature suggests a defect in an early vascular maintenance program

Anti-PECAM immunostained E9.5 KLF2/KLF4 DKO whole-mounts showed apparently normal capillary development and possible rostral to caudal narrowing of the posterior cardinal vein. While E10.5 KLF2-/-KLF4-/-, E10.5 KLF2-/-KLF4+/-, E9.5 KLF2-/-KLF4-/-, and E9.5 KLF2-/-KLF4+/- embryos exhibited a phenotype of variable severity, the pre-formed vessels showed no obvious signs of stalled growth or malformation. In fact, the localized hemorrhaging along the PHV extending to the rostral end of the anterior cardinal vein was the only obvious morphological deficit that was observed.

In adult mice, blood vessels are supported in part by vascular smooth muscle that provides strength and contractility. Interestingly, this tissue responds to signals from its neighboring inner endothelial layer, after exposure to a variety of chemical or physical stimuli (Reviewed by Furchgott, 1983). In embryos, the primitive vascular network is supported by mesenchyme, the undifferentiated connective tissue that will ultimately differentiate into vascular smooth muscle cells during development (Reviewed by Nehls, 1993). No difference was observed in cell density at E9.5 along the primary head vein, where the hemorrhaging occurred. However, E10.5 FVB/N KFL2-/- embryos were recently demonstrated through alcian blue staining to have reduced glycosaminoglycans (GAGs) in the cardiac jelly, situated in the connective tissue of the developing heart (Chiplunkar, unpublished data). GAGs form an integral part of the extracellular matrix (ECM), contributing to the ground substance which

cushions and supports the embryo through an extra-cellular framework (Ross, 2006). It is possible that a reduction in GAGs or other ECM proteins along the PHV may cause the localized hemorrhaging.

Alternatively, as KLF2 was localized to the PHV endothelial cells at E10.5, and KLF4 has been shown to have a role in HUVEC cells (Yet, 1998; McCormick, 2001; Chiambaretta, 2004), it may be possible that the phenotype seen in KLF2/KLF4 DKOs is a result of genetic interactions confined to endothelial cells. It is somewhat striking that multiple KLF2/KLF4 DKOs exhibit hemorrhaging in the same portion of the PHV near the optic vesicle. This population of endothelial cells may be specialized in a way that predisposes them to disruption, given that the fates of endothelial cells are at least partially determined by their microenvironments (Cleaver, 2003).

KLF4 has a vascular role in early embryonic development

Previously, no vascular phenotype has been reported for KLF4-/- *in utero*. KLF2/KLF4 DKO mice demonstrate that KLF4 plays a role in vascular development that is supplemented by the participation of KLF2. Recently, adult KLF4 conditional knockout mice were created as previously discussed via a tamoxifen/Cre-ERt system. Here, these conditional KLF4-/- adult mice displayed thickened arterial intima of the carotid arteries following injury via dissection and ligation (Yoshida, 2008). This phenotype supports the narrative whereby KLF4 maintains the integrity of the vessel, possibly through anti-inflammatory processes. *In vitro* studies have demonstrated that KLF4 activates downstream anti-inflammatory processes, in a role analogous to KLF2 (Topper, 1996; Gimbrone, 2000; Hamik; 2007). Additionally, as demonstrated by the

qRT-PCR assay, KLF4 has a role in the regulation of eNOS, a regulator of vascular smooth muscle tone.

Embryos lacking KLF2 and KLF4 may be unable to withstand the effect of shear stress forces

Shear stress has been repeatedly implicated in the upregulation of KLF2 and KLF4 *in vitro*. KLF2 is upregulated in response to shear stress via a MEK5/ERK5/MEF2 signaling pathway (Parmar, 2005). A recent study demonstrated that MEF2, an activator of KLF2, is derepressed through the phosphorylation and subsequent nuclear export of histone deacetylase 5 via calmodulin-dependent kinase(s), leading to upregulation of KLF2 and direct activation of downstream effectors, such as eNOS (Wang, 2010). On first glance, shear stress may not rank high as a likely player in PHV disruption as it is much higher in the arterial versus the venous branch of the vascular system. Nevertheless, as vasculature begins forming at about E8.5 and the heart starts beating, young arteries and veins are morphologically indistinguishable at E9.5, unlike their adult counterparts which have differing thickness and functional layers to efficiently circulate blood and perfuse tissues.

Dual gene regulation orchestrated by KLF2 and KLF4

EKLF and KLF2 are important for the normal expression of the mouse embryonic β-gobin genes, βh-1 and Ey (Basu, 2007). Recent work using ChIP assays has demonstrated that EKLF and KLF2 bind to the Ey promoter in E10.5 primitive erythroid cells (Alhashem, unpublished data). KLF2 and KLF4 have the same potential to bind to the promoters or enhancers of specific vascular maintenance genes, as suspected by their regulation of the eNOS gene. E11.5 Tie-2 conditional KLF2 knockout mice failed to show decreased eNOS expression

compared to WT mice (Lee, 2006), as do KLF2-/- embryos in our study. These results support the hypothesis that eNOS expression in the absence of KLF2 is rescued by KLF4. While only a small sub-portion of genes were tested in this study, other candidates include the following: THBD, Tie-2, Adm, Ang-1, EphB4, Efnb2, Edn1, Jag1, Notch1, Notch4, NRP1, NRP2, PDGFα, PDGFβ, PDGFRα, PDGFRβ, Scl, TGFβ-1, Tie-1, VEGF, VEGFR2, VEGFR3, the majority of which are exclusively expressed in endothelial cells. Molecularly, the nature of the KLF2-KLF4 gene interaction depends on the localization KLF2 and KLF4 in embryo tissue. KLF2 has been documented in embryo endothelial cells at E9.5 (Kuo, 1997) and was found to be expressed in the endothelium of the PHV at E10.5. KLF4 has been documented as expressed in cranial epithelium and mesenchyme at E10.5, but numerous studies have documented its expression in response to shear stress in HUVEC culture (Yet, 1998; McCormick, 2001; Chiambaretta, 2004). If the nature of the KLF2 and KLF4 gene interaction(s) that contribute to the phenotype occurs in only endothelial cells, then direct regulation of a shared set of downstream genes by KLF2 and KLF4 is a high possibility (Figure 21A). Whereas, if the phenotype is due to ablation of KLF2 in endothelial cells and KLF4 in mesenchymal cells, this would suggest that there is an unidentified interaction of the downstream effectors that is contributing to the early embryonic death (Figure 21B).

Future Directions

In summary, the phenotype observed prior to embryonic death in KLF2/KLF4 DKO mice suggests that KLF2 and KLF4 act as regulators on a shared set of downstream effectors that have roles in vascular maintenance in or surrounding the primary head vein. Future studies to elucidate the molecular mechanism leading to this phenotype may include several of the

following experimental approaches. As the list of potential shared KLF2 and KLF4 gene targets is quite long, additional testing of mRNA levels using qRT-PCR should be attempted for the genes previously listed. As KLF2 appears to be the greater contributor to embryonic death, this implies that it regulates additional gene targets that have roles in vascular maintenance. Previous microarray data identifies potential KLF2 and KLF4 regulated genes in HUVEC culture (Villarreal, 2009; Boon, 2010). Alternatively, a microarray approach using E9.5 whole embryo with KLF2 and KLF4 gene knockout combinations would produce a list reflecting *in vivo* gene interactions from which candidates may be selected. Follow-up studies can also include testing of possible direct regulation of the eNOS gene through a ChIP and a luciferase reporter assay. Alternatively, if one or multiple VEGF receptors are regulated by KLF2 and/or KLF4, this might indicate the source of the filopodial-like cytoplasmic projections of endothelial cells of the PHV in KLF2/KLF4 DKOs. KLF4 conditional knockout mice, with KLF4 ablated in either endothelial or mesenchymal cells may answer the question concerning the nature of the KLF2 and KLF4 gene interaction.

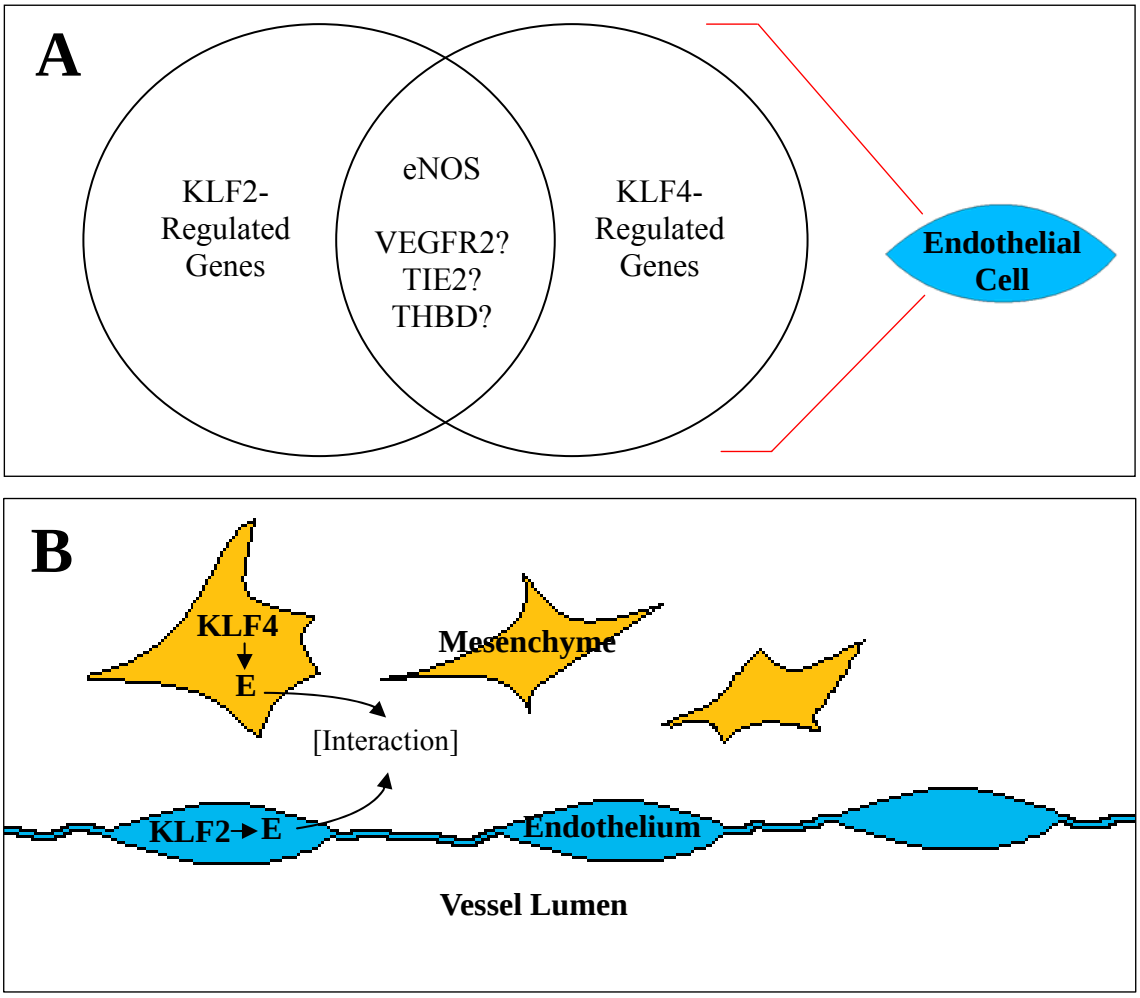

Figure 21: Models of gene regulation by KLF2/KLF4. The above figures postulate how KLF2 and KLF4 interact. In the endothelial cell model, KLF2 and KLF4 drive expression of a shared set of downstream effectors (A). In the mesenchymal-endothelial cell model, KLF2 and KLF4 are expressed in two tissue types and their shared targets generator effector molecules interact through an unspecified mechanism (B).

References

Literature Cited

Abbott, N.J. Astrocyte-endothelial interactions and blood brain barrier permeability. J. Anatomy *200*, 629-638.

Aird, W.C. *et al*. (1997) Vascular bed-specific expression of an endothelial cell gene is programmed by the tissue microenvironment. J. Cell Biology *138*, 1117-1124.

Anderson, P.K., Kern, C.B., Crable, S.C., Lingrel, J.B. (1995) Isolation of a Gene Encodeing a Functional Zinc Finger Protein Homologous to Erythroid Krüppel-Like Factor: Identification of a New Multigene Family. Molecular and Cellular Biology *15*, 5957-5965.

Basu, P., Lung, T.K., Lemsaddek, W., Sargent, T.G., Williams, D.C., Basu, M., Redmond, L.C., Lingrel, J.B., Haar, J.L., Lloyd, J.A. (2007) EKLF and KLF2 have compensatory roles in embryonic β-globin gene expression and primitive erythropoiesis. Blood *110*, 3417-3425.

Basu, P., Sargent, T.G., Redmond, L.C., et al. (2004) Evolutionary conservation of KLF transcription factors and functional conservation of human gamma-globin gene regulation in chicken. Genomics *84*, 311-319.

Benedito, R., Roca, I., Adams, S., Gossler, A., Fruttiger, M., Adams, R. (2009) The notch ligands dll4 and jagged1 have opposing effects on angiogenesis. Cell *137*, 1124-1135.

Bhattacharya, R., SenBanerjee, S., Lin, Z., Mir, S., Hamik, A., Wang, P., Mukherjee, P., Mukhopadhyay, D., Jain, M.K. (2005) Inhibition of vascular permeability factor/vascular endothelial growth factor-mediated angiogenesis by the kruppel-like factor KLF2. J. Biol. Chem. *280*, 28848-28851.

Bieker, J. (2001) Krüppel-Like Factors: three fingers in many pies. The Journal of Biological Chemistry *276*, 34355-34358.

Bieker, J., Southwood, C. (1995) The erythroid krüppel-like factor transactivation domain is a critical component for cell-specific inducibility of a β-globin promoter. Molecular and Cellular Biology *15*, 852-860.

Boon, R.A., Leyen, T.A., Fontijn, R.D., Fledderus, J.O., Baggen, J.M.C., Volger, O.L., van Nieuw Amerongen, G.P., Horrevoets, A.J.G. (2010) Klf2-induced actin shear fibers control both alignment to flow and JNK signaling in vascular endothelium. Blood *115*, 2533-2542.

Brown, R.S., Sander, C., Argos, P. (1985) The primary structure of transcription factor TFIIIA has 12 consecutive repeats. FEBS Lett. *186*, 271-274.

Carmeliet, P. (2000) Mechanisms of angiogenesis and arteriogenesis. Nature Medicine *6*, 389-395.

Chen, Z., Lei, T., Chen, X., Zhang, J., Yu, A., Long, Q., Long, H., Jin, D., Gan, L., Yang, G. (2009) Porcine klf gene family: structure, mapping, and phylogenetic analysis. Genomics *95*, 111-119.

Chiambaretta, F., De Graeve, F., Turet, G., Marceau, G., Gain, P., Dastugue, B., Rigal, D., Sapin, V. (2004) Cell and tissue specific expression of human krüppel-like transcription factors in human ocular surface. Mol. Vis. *10*, 901-909.

Choi, K. (2002) The Hemangioblast: a Common Progenitor of Hematopoietic and Endothelial Cells. Journal of Hematotherapy and Stem Cell Research *11*, 91-101.

Cleaver, O., Melton, D.A. (2003) Endothelial signaling during development. Nature Medicine *9*, 661-668.

Conkright, M.D., Wani, M.A., Lingrel, J.B. (2001) Lung kruppel-like factor contains an autoinhibitory domain that regulates its transcriptional activation by binding WWP1, an E3 ubiquitin ligase. J. Biol. Chem. *276*, 29299-29306.

Crossley, M., Whitelaw, E., Perkins, A., Williams, Y., Fuiwara, Orkin, S.H. (1996) Isolation and characterization of the cDNA encoding BKLF/TEF-2, a major CACCC-box-binding protein in erythroid cells and selected other cells. Mol. Cell. Biol ***16***, 1695–1705.

Cumano, A., Ferraz, J.C., Klaine, M., Di Santo, J.P., Godin, I. (2001) Intraembryonic, but not yolk sac hematopoietic precursors, isolated before circulation, provide long-term multilineage reconstitution. Immunity *15*, 477-485.

Cunningham, D.J., et al. (1902) Textbook of Anatomy. William Wood and Company.

Dang, D.T., Pevsner, J., Yang, V.W. (2000) The biology of mammalian krüppel-like family of transcription factors. Int. Journal of Biochemistry and Cell Biology *32*, 1103-1121.

Das, H., Kumar, A., Lin, Z., Patino, W.D., Hwang, P.M., Feinberg, M.W., Majumder, P.K., Jain, M.K. (2006) Kruppel-like factor 2 (klf2) regulates proinflammatory activation of monocytes. PNAS *103*, 6653-6658.

Davis, S., *et al*. (1996) Isolation of angiopoietin-1, a ligand for the TIE2 receptor, by secretion-trap expression cloning. Cell *87*, 1161-1169.

Dekker, R.J., van Soest, S., Fontijn, R.D., Salamanca, S., de Groot, P.G., VanBavel, E., Pannekoek, H., Horrevoets, A.J.G. (2002) Prolonged fluid shear stress induces a distinct set of endothelial cell genes, most specifically lung krüppel-like factor (klf2). Blood, *100*, 1689-1698.

Dekker, R.J., van Thienen, J.V., Rohlena, J., de Jager, S.C., Elderkamp, Y.W., Seppen, J., de Vries, C.J.M., Biessen, E.A.L, van Berkel, T.J.C., Pannekoek, H., Horrevoets, A.J.G. (2005) Endothelial *klf2* links local arterial shear stress levels to the expression of vascular tone-regulating genes. American J. of Pathology *167*, 609-618.

De Smet, F., Segura, I., De Bock, K., Hohensinner, P.J., Carmeliet, P. (2009) Mechanisms for vessel branching. Filopodia on endothelial tip cells lead the way. Arterioscler Thromb Vasc Biol *29*, 639-649.

Dickson M.C., Martin, J.S., Cousins, F.M. Kulkarni, A.B., Karlsson, S., Akhurst, R.J. (1996) Defective haematopoiesis and vasculogenesis in transforming growth factor-β1 knock out mice. Development *121*, 1845-1854.

Nehls, V., Drenckhahn, D. (1993) The versatility of microvascular pericytes: from mesenchyme to smooth muscle? Histochemistry and Cell Biology *99*, 1-12.

Eichmann, A., Yuan, L., Moyon, D., Lenoble, F., Pardanaud, L., Breant, C. (2005) Vascular development: from precursor cells to branched arterial and venous networks. Int. J. Dev. Biol. *49*, 259-267.

Ehlermann, J., Pfisterer, P., Schorle, H. (2003) Dynamic expression of krüppel-like factor 4 (klf4), a target of transcription factor ap-2α during murine mid-embryogenesis. Anat Rec A Discov Mol Cell Evol Biol. *273*, 677-680.

Evans, P.M., Chen, X., Zhang, W., Liu, C. (2010) Klf4 interacts with β-catenin/TCF4 and blocks p300/CBP recruitment by β-catenin. Molecular and Cellular Biol. *30*, 372-381.

Feinberg, M.W., Wara, A.K., Cao, Z., Lebedeva, M.A., Rosenbauer, F., Iwasaki, H., Hirai, H., Katz, J.P., Haspel, R.L., Gray, S., Akashi, K., Segre, J., Kaestner, K.H., Tenen, D.G., Jain, M.K. (2007) The kruppel-like factor KLF4 is a critical regulator of monocyte differentiation. EMBO Journal *26*, 4138-4148.

Fong, G., Rossant, J., Gertsenstein, M., Breitman, M.L. (1995) Role of Flt-1 receptor tyrosine kinase in regulating the assembly of vascular endothelium. Nature *376*, 66-70.

Fraser, S.T., Isern, J., Baron, M.H. (2007) Maturation and enucleation of primitive erythroblasts during mouse embryogenesis is accompanied by changes in cell-surface antigen expression. Blood *109*, 343-352.

Furchgott, R.F. (1983) Role of endothelium in responses to vascular smooth muscle. Circulation Research *53*, 557-573.

Gerhardt, H., Golding, M., Fruttiger, M., Ruhrberg, C., Lundkvist, A., Abramsson, A., Jeltsch, M., Mitchell, C., Alitalo, K., Shima, D., Betsholtz, C. (2003) VEGF guides angiogenic sprouting utilizing endothelial tip cell filopodia. J. Cell Biol. *161*, 1163-1177.

Gerritsen, M.E. Functional heterogeneity of vascular endothelial cells. Biochem. Pharmacol. *36*, 2701-2711.

Gimbrone, M.A., Topper, J.N., Nagel, T., Anderson, K.R., Garcia-Cardena, G. (2000) Endothelial Dysfunction, Hemodynamic Forces, and Atherogenesis. Ann. N. Y. Acad. Sci. *902*, 230-240.

Gray, H. (1923) Anatomy of the human body. Lea and Febiger.

Haaland, R.E., Yu, W., Rice, A.P. (2005) Identification of LKLF-regulated genes in quiescent $CD4^+$ T lymphocytes. Molecular Immunology *42*, 627-641.

Haar, J.L., Ackerman, G.A. (1970) A phase and electron microscopic study of vasculogenesis and erythropoiesis in the yolk sac of the mouse. Anat. Rec. *170*, 199-223.

Hamik, A., Lin, Z., Kumar, A., Balcells, M., Sinha, S., Katz, J., Feinberg, M.W., Gerszten, R.E., Edelman, E.R., Jain, M.K. (2007) Kruppel-like factor regulates endothelial inflammation. J. Biol. Chem. *282*, 13769-13779.

Hirschi, K.K., Rohovsky, S.A., D'Amore, P.A. (1998) PDGF, TGF-β, and heterotypic cell-cell interactions mediate endothelial cell-induced recruitment of 10T1/2 cells and their differentiation to a smooth muscle fate. J. Cell Biol. *141*, 805-814.

Hoffman, J.I.E., Kaplan, S. (2002) The incidence of congenital heart disease. Journal of American College of Cardiology *39*, 1890-1900.

Huddleson, J.P., Srinivasan, S., Ahmad, N., Lingrel, J.B. (2004) Fluid shear stress induces endothelial KLF2 gene expression through a defined promoter region. Biol. Chem. *385*, 723-729.

Huddleson, J.P., Ahmad, N., Srinivasan, S., Lingrel, J.B. (2005) Induction of klf2 by fluid shear stress requires a novel promoter element activated by a phosphatidylinositol 3-kinase-depedent chromatin-remodeling pathway. J. Biol. Chem. *280*, 23371-23379. `

Jiang, J. Chan, Y., Loh, Y., Cai, J., Tong, G., Lim, C., Robson, P., Zhong, S., Ng, H. (2008) A core Klf circuitry regulates self-renewal of embryonic stem cells. Nature Cell Biol. *10*, 353-360.

Katz, J.P., Perreault, N., Goldstein, B.G., Actman, L., McNally, S.R., Silberg, D.G., Furth, E.E., Kaestner, K.H. (2005) Loss of klf4 in mice causes altered proliferation and differentiation and precancerous changes in adult stomach. Gastroenterology *128*, 935-945.

Kaufmann, M.H. (1992) The atlas of mouse development. Elsevier Ltd. Revised Ed 1998, 92.

King, K.E., Iyemere, V.P., Weissberg, P.L., Shanahan, C.M. (2003) Krüppel-like factor 4 (klf4/gklf) is a target of bone morphogenetic proteins and transforming growth factor β1 in the regulation of vascular smooth muscle cell phenotype. Journal Biol. Chem. *278*, 11661-11669.

Kmiec, Z. Cooperation of liver cells in health and disease. Adv. Anat. Embryol. Cell Biol. *161*, III-XIII, 1-151.

Kuo, C.T., Veselits, M.L., Barton, K.P., Lu, M.M., Clendenin, C., Leiden, J.M. (1997) The LKLF Transcription Factor is Required for Normal Tunica Media Formation and Blood Vessel Stabilization During Murine Embryogenesis. Genes and Development *11*, 2996-3006.

Kuo, C.T., Veselits, M.L., Leiden, J.M. (1997) LKLF: A Transcriptional Regulator of Single-Positive T Cell Quiescence and Survival. Science *277*, 1986-1990.

Lee, J.S., Yu, Q., Shin, J.T., Sebzda, E., Bertozzi, C., Chen, M., Mericko, P., Stadfeld, M., Zhou, D., Cheng, L., Graf, T., MacRae, C.A., Lepore, J.J., Lo, C.W., Kahn, M.L. (2006) Klf2 is an essential regulator of vascular hemodynamic forces in vivo. Dev. Cell *11*, 845-857.

Leveen, P. *et al*. (1994) Mice deficient for PDGF B show renal, cardiovascular, and hematological abnormalities. Genes Dev. *8*, 1875-1887.

Lindahl, P., Johansson, B.R., Leveen, P., Betsholtz, C. (1997) Pericyte loss and microaneurysm formation in PDGF-B deficient mice. Science *277*, 242-245.

Liu, Y., Sinha, S., McDonald, O.G., Shang, Y., Hoofnagle, M.H., Owens, G.K. (2005) Kruppel-like factor 4 abrogates myocardin-induced activation of smooth muscle gene expression. J. Biol. Chem. *280*, 9719-9727.

Loscalzo, J., Schafer, A. (2003) Thrombosis and hemorrhage. Lippincott Williams & Wilkins. 3rd Ed, 306-314.

Lung, T.K. (2008) Analysis of mouse eklf/klf2 E9.5 double knockout: yolk sac morphology and embryonic erythroid maturation. Masters Thesis. VCU Digital Achieves 42-45.

Mack, P.J., Zhang, Y., Chung, S., Vickerman, V., Kamm, R.D., García-Cardeña, G. (2008) Biomechanical regulation of endothelium-dependent events critical for adaptive remodeling. J. Biol. Chem. *284*, 8412-8420.

Maisonpierre, P.C., Suri, C., Jones, P.F., Bartunkova, S., Wiegand, S.J., Radziejewski, C., Compton, D., McClain, J., Aldrich, T.H., Papadopoulos, N., Daly, T.J., Davis, S., Sato, T.N., Yancopoulos, G.D. (1997) Angiopoietin-2, a natural antagonist for Tie2 that disrupts angiogenesis. Science *277*, 55-60.

Matsumoto, N., Laub, F., Aldabe, R., Zhang, W., Ramirez, F., Yoshida, T., Terada, M. (1998) Cloning the cDNA for a new human zinc finger protein defines a group of closely related kruppel-like transcription factors. J. Biol. Chem. ***273,*** 28229–28237.

McCormick, S., Eskin, S., McIntire, L., Teng, C., Lu, C., Russel, C., Chittur, K. (2001) DNA microarray reveals changes in gene expression of shear stressed human umbilical vein endothelial cells. Proc. Natl. Acad. Sci. USA. *98*, 8955-8960.

Meadows, S.M., Salanga, M.C., Krieg, P.A. (2009) Krüppel-like factor 2 cooperates with the ETS family protein ERG to activate *fkl1* expression during vascular development. Development *136*, 1115-1125.

Miller, J., McLachlan, A.D., Klug, A. (1985) Repetitive zinc-binding domains in the protein transcription factor IIIA from Xenopus oocytes. EMBO J. *4*, 1609-1614.

Murray, P. (1932) The Development in Vitro of Blood in the Early Chick Embryo. Proc Roy. Soc. *111,* 497-521.

Mukouyama, Y.S., Shin, D., Britsch, S., Taniguchi, M., Anderson, D.J., (2002) Sensory nerves determine the pattern of arterial differentiation and blood vessel branching in the skin. Cell *109*, 693-705.

Ng, Y.S., Rohan, R., Sunday, M.E., Demello, D.E., D'Amore, P.A. (2001) Differential expression of VEGF isoforms in mouse during development and in the adult. Developmental Dynamics *220*, 112-121.

Nishikawa, S.I., Nishikawa, S., Hirashima, M., Matsuyoshi, N., Kodama, H. (1998) Progressive lineage analysis by cell sorting and culture identities FLK1+VE-cadherin+ cells at a diverging point of endothelial and hemopoietic lineages. Development *112*, 1363-1371.

Norman, B., Davis, J., Piatigorsky, J. (2004) Postnatal Gene Expression in the Normal Mouse Cornea by SAGE. Investigative Opthalmology Vis. Sci. *45*, 429-440.

Orr, F.W., Wang, H.H., Lafrenie, R.M., Scherbarth, S., Nance, D.M. (2000) Interactions between cancer cells cand the endothelium in metastasis. Journal of Pathology *190*, 310-329.

Pabo, C.O., Peisach, E., Grant, R.A. (2001) Design and Selection of Novel Cys_2His_2 Zinc Finger Proteins. Annual Review of Biochemistry *70*, 313-340.

Parmar, K.M., Larman, H.B., Guohao, D., Zhang, Y., Wang, E.T., Moorthy, S.N., Kratz, J.R., Lin, Z., Jain, M.K., Gimbrone, M.A., García-Cardeña, G. (2006) Integration of flow-dependent endothelial phenotypes by kruppel-like factor 2. J. Clin. Invest. *116*, 49-58.

Parmar, K.M., Nambudiri, V., Dai, G., Larman, H.B., Gimbrone, M.A., García-Cardeña, G. (2005) Statins exert endothelial atheroprotective effects via the klf2 transcription factor. J. Biol. Chem. *29*, 26714-26719.

Pasqualini, R., Arap, W., McDonald, D.M. (2002) Probing the structural and molecular diversity of tumor vasculature. Trends. Mol. Med. *8*, 563-571.

Pearson, R., Fleetwood, J., Eaton, S., Crossley, M., Bao, S. (2008) Krüppel-like transcription factors: a functional family. Int. Journal of Biochemistry and Cell Biology *40*, 1996-2001.

Pepper, M.S. (1997) Transforming growth factor-beta: vasculogenesis, angiogenesis, and vessel wall integrity. Cytokine and Growth Factor Reviews *8*, 21-43.

Philipsen, S., Suske, G. (1999) A tale of three fingers: the family of mammalian Sp/XKLF transcription factors. Oxford University Press *27*, 2991-3000.

Risau, W. (1997) Mechanisms of Angiogenesis. Nature *386*, 671-674.

Roberts, W.G., Palade, G.E. (1995) Increased microvascular permeability and endothelial fenestration induced by vascular endothelial growth factor. J. Cell Science *108*, 2369-2379.

Ross, M., Pawlina, W. (2006) Histology: a text and atlas. Lippincott Williams & Wilkins. 5th Ed 2006, 161-164.

Rowland, B.D., Bernards, R., Peeper, D.S. (2005) The KLF4 tumour suppressor is a transcriptional repressor of p53 that acts as a context-dependent oncogene. Nat Cell Biol. *7*, 1074-1082.

Sato, T.N., Tozawa, Y., Deutsch, U., Wolburg-Buchholz, K., Fujiwara, Y., Gendron-Maguire, M., Gridley, T., Wolburg, H., Risau, W., Qin, Y. (1995) Distinct roles of the receptor tyrosine kinases Tie-1 and Tie-2 in blood vessel formation. Nature *376*, 70-74.

SenBanerjee, S., Lin, Z., Atkins, G.B., Greif, D.M., Rao, R.M., Kumar, A., Feinberg, M.W., Chen, Z., Simon, D.I., Luscinskas, F.W., Michel, T.M., Gibrone, M.A., García-Cardeña, G., Jain, M.K. (2004) Klf2 is a novel transcriptional regulator of endothelial proinflammatory activation. J. Exp. Med. *199*, 1305-1315.

Segre, J.A., Bauer, C., Fuchs, E. (1999) Klf4 is a transcription factor required for establishing the barrier function of skin. Nature *22*, 356-360.

Shalaby, F., Rossant, J., Yamaguchi, T.P., Gertsenstein, M., Wu, W., Breitman, M.L., Schuh, A. (1995) Failure of blood-island formation and vasculogenesis in flk-1-deficient mice. Nature, *376*, 62-66.

Shields, J.M., Christy, R.J., Yang, V.W. (1996) Identification and characterization of a gene encoding a gut-enriched krüppel -like factor expressed during growth arrest. J. Biol. Chem. *271*, 20009-20017.

Shinbrot, E., Peters, K.G., Williams, L.T. (1994) Expression of the platelet-derived growth factor β receptor during organogenesis and tissue differentiation in the mouse embryo. Developmental Dynamics *199*, 169-175.

Sissman, N. (1970) Developmental landmarks in cardiac morphogenesis. Comparative chronology. Am. J. Cardiol. *25*, 141-148.

Stewart, P.A., Wiley, M.J. (1981) Developing nervous tissue induces formation of blood-brain barrier characteristics in invading endothelial cells: a study using quail-chick transplantation chimeras. Dev. Biol. *84*, 183-192.

Stone, J., *et al*. (1995) Development of retinal vasculature is mediated by hypoxia induced vascular endothelial growth factor (VEGF) expression by neuroglia. Journal of Neuroscience *15*, 4738-4747.

Swamynathan, S.K., Katz, J.P., Kaestner, K.H., Ashery-Padan, R., Crawford, M.A., Piatigorsky, J. (2007) Conditional deletion of the mouse *klf4* gene results in corneal epithelial fragility, stromal edema, and loss of conjunctival goblet cells. Molecular and Cell Biology *27*, 182-194.

Suri, C. *et al*. (1996) Requisite role of angiopoietin-1, a ligand for the TIE2 receptor, during embryonic angiogenesis. Cell *87*, 1171-1180.

Suske, G., Bruford, E., Philipsen, S. (2005) Mammalian sp/klf transcription factors: bring in the family. Genomics *85*, 551-556.

Thom, T., *et al.* (2006) Heart Disease and Stroke Statistics—2006 Update. Circulation *113*, 85-151.

Topper, J.N., Cai, J., Falb, D., Gimbrone, M.A. (1996) Identification of vascular endothelial genes differentially responsive to fluid mechanical stimuli: cyclooxygenase-2 manganese superoxide dismutase, and endothelial cell nitric oxide synthase are selectively up-regulated by steady laminar shear stress. Proc. Natl. Acad. Sci. U.S.A. *93*, 10417-10422.

Van Thienen, J.V., Fledderus, J.O., Dekker, R.J., Rohlena, J., van IJzendoorn, G.A., Koostra, N.A., Pannekoek, H., Horrevoets, A.J.G. (2006) Shear stress sustains atheroprotective endothelial KLF2 expression more potently than statins through mRNA stabilization. Cardiovascular Research *72*, 231-240.

Villarreal, G., Zhang, Y., Larman, H.B., Gracia-Sancho, J., Koo, A., Garcia-Cardeña, G. (2009) Defining the regulation of KLF4 expression and its downstream transcriptional targets in vascular endothelial cells. Biochemical and Biophysical Research Communications *391*, 984-989.

Wang, H.U., Chen, Z.F., Anderson, D.J. (1998) Molecular distinction and angiogenic interaction between embryonic arteries and veins revealed by ephrin-B2 and its receptor Eph-B4. Cell *93*, 741-753.

Wang, W., Hoon Ha, C., Sook Jhun, B., Wong, C., Jain, M.K., Jin, Z. (2010) Fluid shear stress stimulates phosphorylation-dependent nuclear export of HDAC5 and mediates expression of KLF2 and eNOS. Blood *115*, 2971-2979.

Wani, M.A., Means, R.T., Lingrel, J.B. (1998) Loss of LKLF function results in embryonic lethality in mice. Transgenic Research *7*, 229-238.

Wani, M.A., Wert, S.E., Lingrel, J.B. (1999) Lung kruppel-like factor, a zinc finger transcription factor, is essential for normal lung development. J. Biol. Chem. *274*, 21180-21185.

Warnes, C.A., Liberthson, R., Danielson, G.K., Dore, A., Harris, L., Hoffman, J.I.E., Somerville, J., Williams, R.G., Webb, G.D. (2001). Task force 1: the changing profile of congenital heart disease in adult life. Journal of American College of Cardiology *37,* 1170-1175.

Warot, X., Fromental-Ramain,C., Fraulob, P., Chambon, P., Dolle, P. (1997) Gene dosage-dependent effects of Hoxa-13 and Hoxd-13 mutations on morphogenesis of the terminal parts of digestive and urogenital tracts. Development *124*, 4781- 4791.

Wu, J., Srinivasan, S.V., Neumann, J.C., Lingrel, J.B. (2005) The klf2 transcription factor does not affect formation of preadipocytes but inhibits their differentiation into adipocytes. Biochemistry *44*, 11098-11105.

Wu, J. Bohanan, C.S., Neumann, J.C., Lingrel, J.B. (2008) KLF2 transcription factor modulates blood vessel maturation through smooth muscle cell migration. J. Biol. Chem. *283*, 3942-3950.

Xue, Y., Gao, X., Lindsell, C., Norton, C., Chang, B., Hicks, C., Gendron-Maguire, M., Rand, E., Weinmaster, G., Gridley, T. (1999) Embryonic lethality and vascular defects in mice lack the notch ligand jagged1. Human Mol. Genet. *8*, 723-730.

Yan, F., Liu, Y., Liu, Y., Zhao, Y. (2008) KLF: A novel target for treatment of atherosclerosis. Medical Hypotheses *70*, 845-847.

Yet, S., McA'Nulty, M., Folta, S., Yen, H., Yoshizumi, Hsieh, C., Layne, M., Chin, M., Wang, H., Perrella, M., Jain, M., Lee, M., (1998) Human EZF, a krüppel-like zinc finger protein, is expressed in vascular endothelial cells and contains transcriptional activation domains. J.Biol. Chem. *273*, 1026-1031.

Yoon, H.S., Chen, X., Yang, V.W. (2003) Kruppel-like factor 4 mediates p53-dependent G1/S cell cycle arrest in response to DNA damage. J. Biol. Chem. *278*, 2101-2105.

Yoshida, W., Kaestner, K.H., Owens, G.K. (2008) Conditional deletion of krüppel-like factor 4 delays downregulation of smooth muscle cell differentiation markers but accelerates neointimal formation following vascular injury. Circulation Research *102*, 1548-1557.

Zang, W., Geiman, D.E., Shields, J.M., Dang, D.T., Mahatan, C.S., Kaestner, K.H., Biggs, J.R., Kraft, A.S., Yang, V.W. (2000) The gut-enriched Kruppel-like factor (Kruppel-like factor 4) mediates the transactivating effect of p53 on the p21WAF1/Cip1 promoter. J. Biol. Chem. *275*, 18391-18398.

Zhang, P., Basu, P., Redmond, L.C., Morris, P.E. Rupon, J.W. Ginder, G.D. Lloyd, J.A. (2005) A functional screen for Krüppel-like factors that regulate the human gamma-globin gene through the CACCC promoter element. Blood Cells Mol Dis. *35*, 227-235.

Zheng, B., Han, M., Wen, J. (2010) Role of Krüppel-like factor 4 in phenotypic switching and proliferation of vascular smooth muscle cells. IUBUM Life *62*, 132-139.

Zerwes, H.G., Risau, W. (1994) Polarized secretion of a platelet-derived growth factor-like chemotactic factor by endothelial cells *in vitro*. J. Cell Biol. *105*, 2037-2041.

Appendix

Solutions:

Millonig's Buffer

Solution A

dH_2O	1000 mL
NaH_2PO_4	22.6 g

Solution B

dH_2O	250 mL
NaOH	6.4 g

After dissolving, pour off 170 mL Solution A and replace with an equivalent amount of Solution B.

Vita

Benjamin Christopher Curtis was born on August 30, 1985 in Fairborn, Ohio. He graduated from North Stafford High School in Stafford, Virginia in 2004. He received his Bachelor of Arts in Biology in 2008 from the University of Virginia, in Charlottesville, Virginia.